Aus dem Zentrum für Augenheilkunde der Universität zu Köln
Klinik und Poliklinik für Allgemeine Augenheilkunde
Direktor: Universitätsprofessor Dr. med. C. Cursiefen

Validation of the Portable Next-Generation VECTRA H2 3D Imaging System for Periocular Anthropometry

Inaugural-Dissertation zur Erlangung der Doktorwürde
der Medizinischen Fakultät
der Universität zu Köln

vorgelegt von
Wanlin Fan
aus Anhui, China

promoviert am 30. Juni 2023

Gedruckt mit Genehmigung der Medizinischen Fakultät der Universität zu Köln
Druckjahr：2023

Dekanin/Dekan: Universitätsprofessor Dr. med. G. R. Fink

1. Gutachterin oder Gutachter: Universitätsprofessor Dr. med. Dr. phil. L. M. Heindl
2. Gutachterin oder Gutachter: Privatdozent Dr. med. R. Widder

Erklärung

Ich erkläre hiermit, dass ich die vorliegende Dissertationsschrift ohne unzulässige Hilfe Dritter und ohne Benutzung anderer als der angegebenen Hilfsmittel angefertigt habe; die aus fremden Quellen direkt oder indirekt übernommenen Gedanken sind als solche kenntlich gemacht.[1]

Bei der Auswahl und Auswertung des Materials sowie bei der Herstellung des Manuskriptes habe ich Unterstützungsleistungen von folgenden Personen erhalten:

Universitätsprofessor Dr. med. Ludwig M. Heindl, Dr. med. Alexander C. Rokohl, Dr. med. Yongwei Guo, Dr. med. Konrad R. Koch, Dr. med. Simona Schlereth und Prof. Dr. med. Rafael Grajewski.

Weitere Personen waren an der Erstellung der vorliegenden Arbeit nicht beteiligt. Insbesondere habe ich nicht die Hilfe einer Promotionsberaterin/eines Promotionsberaters in Anspruch genommen. Dritte haben von mir weder unmittelbar noch mittelbar geldwerte Leistungen für Arbeiten erhalten, die im Zusammenhang mit dem Inhalt der vorgelegten Dissertationsschrift stehen.

Die Dissertationsschrift wurde von mir bisher weder im Inland noch im Ausland in gleicher oder ähnlicher Form einer anderen Prüfungsbehörde vorgelegt.

Die dieser Arbeit zugrunde liegenden Daten wurden durch meine Mitarbeit im Zentrum für Augenheilkunde der

Universität zu Köln ermittelt.

Diese Daten wurden von Herrn Universitätsprofessor Dr. med. Ludwig M. Heindl, Herrn Dr. med. Alexander C. Rokohl, Herrn Dr. med. Yongwei Guo, Herrn Dr. med. Konrad R. Koch, Frau Dr. med. Simona Schlereth, Herrn Prof. Dr. med. Rafael Grajewski und von mir zusammen ausgewertet.

Erklärung zur guten wissenschaftlichen Praxis:

Ich erkläre hiermit, dass ich die Ordnung zur Sicherung guter wissenschaftlicher Praxis und zum Umgang mit wissenschaftlichem Fehlverhalten (Amtliche Mitteilung der Universität zu Köln AM 132/2020) der Universität zu Köln gelesen habe und verpflichte mich hiermit, die dort genannten Vorgaben bei allen wissenschaftlichen Tätigkeiten zu beachten und umzusetzen.

Köln, den

Unterschrift: .....

ACKNOWLEDGEMENTS

First, I am so grateful to Prof. Dr. Ludwig M. Heindl for his support and help since I came to Germany. He encouraged me to explore every new idea and supported me in realizing it. When I was confused, he always encouraged me patiently and gave me selfless help. Without his encouragement and support, I could not have completed the project.

I would also like to thank Univ.-Prof. Dr. med. Claus Cursiefen, Director of the Center of Ophthalmology of the University of Cologne, for the opportunity to conduct this program for our international students and for all the facilities and assistance he provided.

A sincere thanks to Dr. med. Alexander C. Rokohl for his generous help and professional and critical advice in the implementation of my project. I would also like to thank all colleagues in our research group, Philomena A. Wawer Matos, Yongwei Guo, Xioayi Hou, Jinhua Liu, Senmao Li, Sitong Ju, Xiaojun Ju, Xueting Li, and Xinceng Hou for their cooperation and help. At the same time, I would like to thank my partners, Patrick Kupka，Julia Maus, Christoph Bechtloff, Leon Collmer, Ann-Christin Dembert for their hard work and translation assistance over the past year and for the warm friendship they have given me.

In addition, I would like to give special thanks to my beloved parents for giving me life and supporting me to pursue my ideals and ambitions. I would also like to thank my dear wife for her constant companionship and support, which allowed me to study in a foreign country without any worries.

Finally, I like to thank all the volunteers who participated in this project for their patient participation and cooperation.

Dedication

To my beloved parents and wife

TABLE OF CONTENTS

ABBREVIATION

En	Endocanthion, inner commissure of the palpebral fissure
Ex	Exocanthion, outer commissure of the lower and upper eyelash roots of the palpebral fissure
Pc	Pupillary center
Lm	Medial corneoscleral limbus point horizontal to pupillary center
Ll	Lateral corneoscleral limbus point horizontal to pupillary center
Em	Inferior margin point of the medial eyebrow end (sometimes locates at the same place with EEn)
Em”	Superior margin point
Em’	Middle point
EEn	Inferior margin point of eyebrow vertical to En
EEn”	Superior margin point of eyebrow vertical to En
EEn’	Middle point of eyebrow vertical to En
Um	Middle point between En and Lm’at the upper palpebral margin on the lash roots
Um’	Middle point between En and Lm” at the lower palpebral margin on the lash roots
FUm	Point vertical to Um at the lid fold superioris
EUm	Point vertical to Um at the inferior margin of eyebrows
EUm”	Point vertical to Um at the superior margin point
EUm’	Point vertical to Um at the middle point
Lm’	Point vertical to Lm at the upper palpebral margin on the lash roots
Lm”	Point vertical to Lm at the lower palpebral margin on the lash roots

FLm Point vertical to Lm at the lid fold superioris

ELm Point vertical to Lm at the inferior margin of eyebrows

ELm” Point vertical to Lm at the superior margin of eyebrows

ELm’ Point vertical to Lm at the middle margin of eyebrows

Ps Palpebrale superioris, Point vertical to Pc at the upper palpebral margin on the lash roots

Pi Palpebrale inferioris, Point vertical to Pc at the lower palpebral margin on the lash roots

FPs Point vertical to Pc at the lid fold superioris

EPs Point vertical to Pc at the inferior margin of eyebrows

EPs” Point vertical to Pc at the superior margin of eyebrows

EPs’ Point vertical to Pc at the middle margin of eyebrows

Ll’ Point vertical to Ll at the upper palpebral margin on the lash roots

Ll” Point vertical to Ll at the lower palpebral margin on the lash roots

FLl Point vertical to Ll at the lid fold superioris

ELl Point vertical to Ll at the inferior margin of eyebrows

ELl” Point vertical to Ll at the superior margin of eyebrows

ELl’ Point vertical to Ll at the middle margin of eyebrows

Ul The middle between Ex and Ll’at the upper palpebral margin on the lash roots

Ul’ The middle between Ex and Ll”at the lower palpebral margin on the lash roots

FUl FUl Point vertical to Ul at the lid fold superioris

EUl Point vertical to Ul at the inferior margin of eyebrows

EUl” Point vertical to Ul at the superior margin of eyebrows

EUl’ Point vertical to Ul at the middle margin of eyebrows

FEx Point vertical to Ex at the lid fold superioris

EEx Point vertical to Ex at the inferior margin of eyebrows

EEx” Point vertical to Ex at the superior margin of eyebrows

EEx’ Point vertical to Ex at the middle margin of eyebrows

FExl Point vertical to Ex at the lid fold superioris in lateral view

EExl Point vertical to Ex at the inferior margin of eyebrows in lateral view

EExl” Point vertical to Ex at the superior margin of eyebrows in lateral view

EExl’ Point vertical to Ex at the middle margin of eyebrows in lateral view

El Inferior margin of the lateral eyebrow end

El” Superior margin of the lateral eyebrow end

El’ Middle margin of the lateral eyebrow end

1. SUMMARY

Our study *Validation of the portable next-generation VECTRA H2 3D imaging system for periocular anthropometry*[1] validates the reliability of the new portable VECTRA H2 for periocular anthropometry. We photographed the same participants separately using the portable VECTRA H2 and the well-validated static device VECTRA M3. Subsequently, we placed landmarks on both photographs using the same periocular standardized 3D landmark positioning protocol. Then 49 periocular parameters were measured separately, namely periocular linear distance, curve, and angle. Finally, the intra- and inter-device reliability were analyzed. The results show that this new portable 3D imaging device, VECTRA H2, has intra-device reliability consistent with that of the static device, VECTRA M3, and slightly lower inter-device reliability, but taking the average of two captures improves inter-device reliability to some extent. The fissure-related and eyebrow-related variables have good intra-device and inter-device reliability. This result provides an essential basis for further applications of the VECTRA H2 device in the periocular region. In the future, this portable device can be used together with static devices to guide periocular surgery planning and assess postoperative outcomes. Different 3d imaging devices can be selected for use in clinical practice depending on the actual situation.

This study is the first to evaluate the reliability of a portable 3D stereophotogrammetric device for periocular measurements. These results may provide the basis for the widespread use of portable devices for periocular 3D stereophotogrammetry. In the future, it may expand the application scenario of 3D imaging systems in clinical practice, thus guiding the diagnosis and treatment of different physicians.

2. DEUTSCHE ZUSAMMENFASSUNG

Titel der Inauguraldisseration:

Validierung des tragbaren VECTRA H2 3D-Bildgebungssystems der nächsten Generation für die periokulare Anthropometrie

von Fan, Wanlin

aus dem Zentrum für Augenheilkunde der Universität zu Köln

Unsere Studie Validation of the portable next-generation VECTRA H2 3D imaging system for periocular anthropometry[1] validiert die Zuverlässigkeit des neuen tragbaren VECTRA H2 für die periokulare Anthropometrie. Wir fotografierten dieselben Probanden getrennt mit dem tragbaren VECTRA H2 und dem gut validierten statischen Gerät VECTRA M3. Anschließend platzierten wir auf beiden Fotos Orientierungspunkte nach demselben standardisierten periokularen 3D-Positionierungsprotokoll. Dann wurden 49 periokulare Parameter separat gemessen, nämlich der periokulare lineare Abstand, die Kurve und der Winkel. Abschließend wurde die Zuverlässigkeit innerhalb des Geräts und zwischen den Geräten analysiert. Die Ergebnisse zeigen, dass dieses neue tragbare 3D-Bildgebungsgerät Vectra H2 eine übereinstimmende Intra-Geräte Zuverlässigkeit mit dem statischen Vectra H3 aufweist. Es zeigt sich jedoch eine etwas geringere Inter-Geräte Zuverlässigkeit, wobei der Durchschnitt von zwei Aufnahmen diese Inter-Geräte Zuverlässigkeit wiederum um einen gewissen Grad verbessert. Die fissur- und augenbrauenbezogenen Variablen haben eine gute Zuverlässigkeit innerhalb des Geräts und zwischen den Geräten. Dieses Ergebnis bildet eine wesentliche Grundlage für weitere Anwendungen des VECTRA H2 Geräts im periokularen Bereich. In Zukunft kann dieses tragbare Gerät zusammen mit statischen Geräten verwendet werden, um die periokulare Operationsplanung zu unterstützen und die postoperativen Ergebnisse zu beurteilen. Je nach Situation können verschiedene 3D-Bildgebungsgeräte für den Einsatz in der klinischen Praxis ausgewählt werden.

Diese Studie ist die erste, die die Zuverlässigkeit eines tragbaren 3D-Stereophotogrammetriegeräts für periokulare Messungen bewertet. Diese Ergebnisse können die Grundlage für den breiten Einsatz von tragbaren Geräten für die periokulare 3D-Stereophotogrammetrie bilden. In Zukunft könnte dies das Anwendungsszenario

von 3D-Bildgebungssystemen in der klinischen Praxis erweitern und so die Diagnose und Behandlung verschiedener Ärzte unterstützen.

3. INTRODUCTION

3.1 Anthropometry of facial soft tissues

Anthropometry (from the Greek Anthropos: human, Metron: measure) is the systematic measurement of physical characteristics of the human body such as weight, size, and shape [2]. This convenient, simple, inexpensive, and non-invasive technique allows the measurement of the size and structure of the human body. It thus reflects the health and nutritional status of the person being measured [3]. Since Farkas developed standardized landmarks for head and facial anthropometry and various metrics for measurement and assessment [4], it is possible to calculate standardized scores for reliable and objective comparisons of surgical procedures, age, and other factors [5-12]. With the development of technology, facial anthropometry has been widely used in various facial procedures, such as orthodontics [13, 14], dental rehabilitation [15], craniofacial [16], and maxillofacial [17-19], facial cosmetic surgery [20], and facial dermatology [21]. Craniofacial soft tissue anthropometry is essential in monitoring average craniofacial growth, assessing facial deformities, developing various surgical plans, and evaluating postoperative outcomes [22-26].

3.2 Different techniques for Anthropometry

Anthropometric methods include traditional direct anthropometry (rulers and calipers) and two-dimensional (2D) photogrammetry and three-dimensional (3D) imaging techniques.

3.2.1 Direct Anthropometry

Direct anthropometry was developed primarily using calipers and rulers. Farkas et al. created an extensive database of direct anthropometric methods that can be used for facial measurements [27]. Direct anthropometry has been considered the standard golden method for facial measurements. However, this method has some disadvantages, such as it is time-consuming and very dependent on the patient's cooperation [28].

3.2.2 Two-dimensional Anthropometry

Two-dimensional imaging techniques were used in anthropometry more than forty years ago [29]. Two-

dimensional images are snapshots of dynamic objects and therefore require the cooperation of participants during image acquisition. 2D imaging is non-invasive, fast, and inexpensive, so it is easier to obtain than direct measurements [30]. Although 2D images have been widely used for facial measurements[31-35], some problems such as magnification, distortion, and variables affect the results (e.g., different object camera distances and lighting conditions) [36]. In addition, this technique can only provide a planar contour analysis of the entire facial 3D structure. It cannot comprehensively analyze the entire facial 3D structure, especially for the evaluation of surface area and volume [37].

3.2.3 Three-dimensional Anthropometry

Three-dimensional (3D) facial imaging systems are the most promising tools for facial soft tissue assessment. Three-dimensional systems have gradually replaced two-dimensional (2D) systems and traditional anthropometric measurements. Three-dimensional imaging technology is taking photos simultaneously through different angles of high-resolution and fast-acquisition cameras and synthesizing them into 3D images. The method allows accurate and non-invasive capture of surface shapes, contours, and colors. In addition, the software that comes with the system allows not only visualization and analysis, but also linear distance, angle, area and volume measurements [38, 39]. The advantages of this method are speed, high color resolution, absence of motion artifacts, and ease of archiving [40, 41]. 3D stereoscopic imaging is now widely used in measuring facial soft tissues, and its accuracy and reliability have been proven [42-44].

3.3 Different devices for Three-dimensional (3D) stereophotogrammetry

So far, the market's standard three-dimensional (3D) imaging systems mainly include VECTRA, Artec EVA, and 3D MD systems [36, 45, 46]. Among the different 3D facial imaging systems, Canfield (Canfield Scientific, Parsippany, NJ, USA) has developed a series of devices called " VECTRA ", which includes both static and portable versions.

3.3.1 Static stereophotogrammetric device

Currently, most devices are static, mainly including VECTRA M3[47, 48], VECTRA M5[49, 50], and VECTRA

XT[51]. Static devices have multiple cameras set up at different angles so that they can capture multiple facial images at the same time. Several studies[47, 50] have compared the linear distance results of the face obtained by static equipment with those obtained by calipers and found no significant differences between the two, which suggests that static 3D stereophotogrammetric imaging systems (VECTRA M3 and M5) have good accuracy and reproducibility in assessing facial anthropology. Furthermore, Verhulst et al. [51] compared the Vectra static device (i.e., Vectra XT) with two other static imaging devices, 3dMDface (3dMD, Atlanta, GA) and Artec Eva (Artec, Luxembourg). They revealed no significant difference in the accuracy of the three systems. However, as static devices are expensive, bulky, and fixed devices that require frequent calibration, this dramatically limits their broader application in clinical and scientific research.

3.3.2 Portable stereophotogrammetric device

The major portable devices are VECTRA H1 and VECTRA H2, the former being the first-generation device and the latter being the latest second-generation device. Due to the advantages of portable devices such as low cost, no need for calibration, to portability, this device has a great prospect of application in the future. The portable devices consist of a DSLR camera and a laptop computer, which are required to acquire three images of the same subject from three different angles in succession, which are then synthesized into a final 3D facial model [52]. Since subjects may change their facial pose between consecutive shots or make unconscious movements, these acquisition systems may show more significant errors in the representation of the final 3D model [53]. For this reason, many studies have compared the results of facial measurements from this device with those obtained with calipers or other static 3D imaging devices. Gabelli et al. [53]compared it with the Vectra M3 for facial angle, area, and volume measurements; Camison et al. [52] compared it with the 3dMD facial system by heat map; Liberton et al. [54] compared the Vectra H1 device with the 3dMD facial system and the ProFace laser scanning system. All studies concluded that the device was accurate and comparable to fixed devices. Although there is some error, it is within the acceptable margin of error for clinical applications.

3.4 Current research on 3D stereophotogrammetry for periocular anthropometry

In recent years, three-dimensional stereophotogrammetry has gradually replaced two-dimensional (2D) systems and traditional anthropometry, especially in craniofacial anthropometry applications[55]. However, anthropometric studies of this system in the periocular region have been more limited. With the development

and validation of the first standardized periocular anthropometric protocol by Guo et al.[56], several studies based on this protocol have successfully demonstrated the high reliability and accuracy of static 3D stereophotogrammetry in the periocular linear distance, curve, angle and area measurements[57-60]. The results of these studies provide a theoretical basis for 3D anthropometric measurements of periocular soft tissue surfaces and contribute to the clinical application of 3D imaging systems in the field of oculoplastics. Nevertheless, no studies have been reported on applying portable 3D stereophotogrammetry equipment for periocular measurements. Furthermore, it is worth mentioning that Vectra devices are constantly being updated and that the portable Vectra H1 imaging system no longer exists and has been replaced by the latest Vectra H2 device. Therefore, validation of a new generation of portable 3D imaging systems for periocular measurements and comparison with static 3D imaging systems plays a crucial role in broadening the application of different 3D imaging systems in eyelid and oculoplastic surgery.

3.5 Aims

The aim of our study on Validation of the portable next-generation VECTRA H2 3D imaging system for periocular anthropometry was to evaluate and compare the reliability of periocular measurements using two different 3d imaging devices: a static device and a portable device, which can provide a feasibility basis for selecting the most suitable 3D stereophotogrammetric device for periocular anthropometry in the future according to the actual situation.

4.Validation of the portable next-generation VECTRA H2 3D imaging system for periocular anthropometry

Wanlin Fan, M.D.[1], Yongwei Guo, M.D.[2], Xiaoyi Hou, M.D.[1], Jinhua Liu, M.D.[1], Senmao Li, M.D.[1], Sitong Ju, M.D.1, Philomena A. Wawer Matos, M.D.1, Michael Simon, M.D.1, Alexander C. Rokohl, M.D.1* †, Ludwig M. Heindl, M.D. 1,3* †

†These authors have contributed equally to this work and share the senior authorship.

[1]Department of Ophthalmology, University of Cologne, Faculty of Medicine and University Hospital Cologne, Cologne 50937, Germany

[2]Eye Center, Second Affiliated Hospital, Zhejiang University School of Medicine, Hangzhou, China

[3]Center for Integrated Oncology (CIO), Aachen-Bonn-Cologne-Duesseldorf, Cologne, Germany

***Correspondence:**

Ludwig M. Heindl

ludwig.heindl@uk-koeln.de

Alexander C. Rokohl

alexander.rokohl@uk-koeln.de

Financial Disclosure

The authors have no financial interest to disclose.

Funding

Supported by State Scholarship Fund from China Scholarship Council.

Short Running Head

3D Imaging in Periocular Anthropometry

4.1 ABSTRACT

Purpose: Portable three-dimensional imaging systems are becoming increasingly common for facial measurement analysis. However, the reliability of portable devices may be affected by the necessity to take three pictures at three time points. The purpose of this study was to evaluate the effectiveness of portable devices for assessing the periocular region.

Methods: In 60 Caucasian volunteers (120 eyes), four facial scans (twice for each instrument) using the portable VECTRA H2 and static VECTRA M3 devices were performed; patients' heads were kept straight, looking ahead, with a neutral facial expression. One assessor set 52 periocular landmarks in the periocular area of each image and subsequently assessed intra- and inter-device reliability by comparing two within-device measurements and one between-device measurement, respectively.

Results: The mean absolute difference (MAD) (0.13 and 0.12 units), relative error of measurement (REM) (0.61% and 0.68%), technical error of measurement (TEM)(1.02 and 0.80 units), relative TEM (rTEM) (5.51% and 4.43%), and intraclass correlation coefficient (ICC) (0.89, 0.89) showed good intra-device reliability for M3 and H2; MAD (0.63, 0.62 units), REM (2.83%, 2.69%), TEM (1.31, 1.10 units), rTEM (7.62%, 5.57%) and ICC (0.79, 0.83) indicated that inter-device reliability deteriorated compared to intra-device reliability and that the inter-device reliability of the first scan (moderate) was lower than that of the average of the two scans (good).

Conclusions: The portable VECTRA H2 device proved reliable in assessing most periocular linear distances, curve distances, and angles; some improvement in inter-device reliability can be achieved by using the average of two scans.

Keywords: three-dimensional anthropometry, portable stereophotogrammetry devices, validity, reliability,

periocular morphology

4.2. INTRODUCTION

The anthropometric data of facial soft tissues are widely used in plastic (1) and craniomaxillofacial surgery (2–4). These data are important to develop surgical plans (5) and assess outcome prognosis (6–8). Particularly, the periocular region plays an important role in facial attractiveness, emotional expression, and differentiation by ethnicity (9, 10), gender, and age (11, 12). It is also a major reference indicator for corrective, restorative, or cosmetic surgery (13). In recent years, non-invasive three-dimensional (3D) surface imaging methods, including VECTRA, Artec EVA, and 3D MD systems (14–16) have gradually replaced traditional direct anthropometric techniques (using rulers and calipers) and two-dimensional (2D) photography. Most of the existing 3D photogrammetry systems are static devices, which prominently feature in capturing photos of participants from three different angles at a single time point and composing a 3D photo using a computer. Previous studies have proposed the first standardized periocular anthropometric protocol (17, 18) and showed potential clinical applications, including a novel standardized lower eyelid tension distraction test and a lateral distraction test (19, 20). The reliability (repeatability) and accuracy of the VECTRA M3 static device is very high for linear, curvilinear, angular, area, and volume measurements (21–25). However, the device is expensive, bulky, untransportable, and requires frequent calibration (2, 14, 26–28) to reach this high reliability, which are considerable limitations, especially for patients who cannot walk independently or reside in remote and poor areas.

Currently, portable 3D imaging devices are available in the market. These systems comprise only one digital single-lens reflex camera in addition to a computer system (5). Due to low cost, no need for calibration, and portability, portable 3D photogrammetry systems have high potential to be used extensively in research and routine clinical measurements in the future. Although several publications have conducted facial analyses using older portable devices (5, 16, 29–31), including studies on the reproducibility of these devices (VECTRA H1) in comparison with static devices (3D MD or VECTRA M3) (5, 31), some issues remain to be addressed. First, the primary portable device used in previous studies was the VECTRA H1; the newest generation, VECTRA H2, was not used. Second, there are no studies on the application of portable devices in the periocular area with newly developed standardized landmarks protocols. Finally, many factors, including head and eye movements, camera movements, user dependence, and facial expressions, may affect the reliability of the portable device during the three shots. Therefore, this study aimed to evaluate the reliability of a novel portable stereophotogrammetric device VECTRA H2 compared to the static VECTRA M3 (the current gold-standard 3D imaging system) for three-dimensional periocular analysis and subsequently provide a basis for the feasibility of

VECTRA H2 in periocular applications.

4.3. METHODS

4.3.1. Study participants

Sixty Caucasian volunteers (30 men and 30 women, 120 eyes) aged 18–48 years (28.2 ± 6.2 years) were recruited for this study. The study sample size was calculated based on the results of the interdevice comparison between M3 and H2 for 10 volunteers in the pre-test study (LCAm: 67.77 ± 10.65 ° vs 62.98 ± 7.09 °). With a 2-sided 5% significance level and 80% power, a sample size of 34 patients per group was determined by PASS software (Version 15, UT, USA). Exclusion criteria were deformities, lesions, surgical, or traumatic events involving the face. All participants signed an informed consent form, and this study was performed in accordance with the principles of the Declaration of Helsinki and approved by the ethics committee of Cologne University (approval no: 17-199).

4.3.2. 3D image acquisition and data collection

Before the images were obtained, all volunteers were asked to remove their makeup, take off their jewelry, and pull their hair back to ensure complete exposure of their forehead and eyebrows. Thereafter, the facial images of each volunteer were captured twice by a static VECTRA M3 and a portable VECTRA H2 system (Canfield Scientific, Inc., Parsippany, NJ, USA). Scanning with both devices was performed consecutively in the same room, and the volunteers sat in a neutral posture. For the static VECTRA M3, calibration was performed according to device guidance before each capture. During acquisition, participants looked at the upper-middle mirror in the machine, keeping their eyes between the vertical and horizontal reference lines on the screen. For the portable VECTRA H2, the operator took three consecutive photographs from three angles as required by the device instructions: the first photograph was taken 30 cm below 45 degrees on the right side of the volunteer's face, and the second photograph was taken with the camera in front of the face. Subsequently, the third picture was taken on the left side of the face at 30 cm below 45 degrees (**Figure 1**). Finally, the computer connected to the camera merged the three photos into one 3D photo using VAM software version 2.8.2 (Canfield Scientific, Inc.).

This study employed 52 3D anthropometric landmarks of the periocular region developed and validated by our

research group (**Figure 2**). The definitions of these landmarks and measurements are detailed in **Tables 1, 2.** Subsequently, the study measured three categories of data (linear distances, curves, and angles).

4.3.3. Statistical Analysis

Statistical analysis was performed using SPSS 23.0 software (Armonk, NY: IBM Corp.), and graphs were created by GraphPad Prism 9 (GraphPad Software, San Diego, CA, USA). Differences in the age distribution of men and women among volunteers were assessed using the Wilcoxon's signed rank-sum test. All measured data were tested for normality using the Kolmogorov-Smirnov test. For data conforming to a normal distribution, paired t-tests were conducted to assess differences within and between devices. For non-normally distributed data, Wilcoxon's signed-rank test was used. P-values <0.05 were considered to indicate statistical significance.

Intra-device reliability was analyzed by comparing the images captured twice by each device (VECTRA M3 and VECTRA H2), and inter-device reliability was analyzed by comparing the metric parameters obtained from the first scan (using VECTRA H2 and VECTRA M3) and the measured average of the images scanned twice with each device. The intraclass correlation coefficient (ICC) has a value between 0 and 1, and a value closer to 1indicates high reliability. ICC values allowed the classification of the agreement into three classes: <0.4, poor agreement; 0.4–0.75, satisfactory; and ≥0.75, excellent (32). Given the small periocular measurements, we set the minimum error threshold for the mean absolute difference (MAD) and technical error of measurement (TEM) to 1 unit (millimeter or degree). Relative error of measurement (REM) and relative TEM (rTEM) values can be classified into five categories (excellent, <1%; very good, 1–3.9%; good, 4–6.9%; moderate, 7–9.9%; and poor,>10%) based on the scale proposed by Camison et al. and Andrade et al. (5, 33).

4.4. RESULTS

The measurement results (means and standard error, SD) of the M3 and H2 system are shown in **Table 3.** Repeatability parameters (ICC, MAD, TEM, REM, and rTEM) within and between the VECTRA M3 and H2 devices are presented in **Tables 4, 5.**

4.4.1. Intra-device reliability with VECTRA M3

ICC **(Table 4, Figure 3)** estimates for most M3 intra-device comparisons were excellent (0.81–1.00), except for two upper lid fold-related variables (FPDI: 0.73, FExDI: 0.70) and one eyelid fissure-related variable (LCAm:

0.68). As shown in **Table 6** and **Figure 4**, MAD was <1 unit for 48 of the 49 parameters, and LCAm was between 1 and 2 units. TEM was <1 unit for 42 parameters (87.5% eyebrow-related variables, 100% upper lid fold-related variables, and 60% palpebral fissure-related variables); the largest measurement error was for the palpebral fissure-related variable MCAm (6.05°). The REM and rTEM results for each comparison are shown in **Figure 5 and Figure 6**. Of seven upper lid fold-related variables, 57.1% of REM values were <1% and 42.9% of values were between 1% and 3.9%. As for rTEM, 71.4% of variables were >10%, except for FExD, which was <7%, and FDPm, which was <10%. FExDI (rTEM = 13.87%) had the largest value. REM was less than 1% for 73.3% of palpebral fissure-related variables, and 26.7% were in the 1–3.9% range. Except for MCAm (rTEM = 8.63%) and LCAm (rTEM = 13.61%), 86.7% of palpebral fissure-related values showed an rTEM <7% (20% of variables were <1%, 46.7% were between 1% and 3.9%, and 20% were between 4% and 6.9%). Moreover, the rTEM and REM of all brow-related variables were <7%. Additionally, 95.8% of REM values were <1%, 75% of rTEM and 4.2% of REM values were between 1–3.9%, and 25% of rTEM values were between 4% and 6.9%.

4.4.2. Intra-device reliability with VECTRA H2

Intra-device ICC **(Table 4, Figure 3)** was above 0.75 for most variables measured by device H2, except for one eyebrow-related parameter (EPDl_M) and three upper lid fold-related variables (FPD, FLl, and FPDl), with an ICC between 0.4 and 0.75. Figure 4 and Table 6 show that all 49 parameters with a MAD and 41 parameters with TEM had a value of <1 unit (87.5% of eyebrow-related variables, 100% of upper lid fold-related variables, and 60% of palpebral fissure-related variables). The largest measurement error was the palpebral fissure-related variable LCAm (4.03°); 28.6% of upper lid fold-related variables showed an REM <1%, 57.1% had variables between 1% and 3.9%, and the maximum value of FPD was 5.163%. All these variables had an rTEM greater than 7%, 28.6% of these variables had an rTEM between 7% and 10%, and 71.4% had an rTEM >10%; the maximum value was FPD (rTEM = 15.76%). All palpebral fissure-related variables showed an REM and rTEM <7% (80% of REM and 26.7% of rTEM values were <1%, 20% of REM and 40% of rTEM values were between 1–3.9%, and 33.3% of rTEM values were between 4% and 6.9%). Except for EPDl_M, ELID_l, and EPD_l with an rTEM greater than 7%, REM and rTEM were <7% across all brow-related variables (87.5% of variables had an REM <1%, 70.8% of rTEM and 12.5% of REM variables were between 1% and 3.9%, and 16.7% of rTEM values were between 4% and 6.9%).

4.4.3. Inter-device reliability between VECTRA H2 and VECTRA M3

When the first captures of both devices (M3 and H2) were used to compare inter-device reliability; 33 variables showed an ICC (**Table 5**) >0.75 (83.3% of brow-related variables and 73.3% of palpebral fissure-related variables), 15 variables had ICC values between 0.4 and 0.75 (16.7% of brow-related variables, 100% of upper eyelid fold-related variables, and 20% of palpebral fissure-related variables). The smallest ICC value was for a palpebral fissure-related variable, LCAm (ICC = 0.39). Forty-one variables had an MAD <1 unit (100% of eyebrow-related variables, 100% of upper eyelid fold-related variables, and 53.3% of palpebral fissure-related variables), and the highest MAD value was for LCAm (6.825°). Twenty-eight measurements had a TEM <1 unit (62.5% of brow-related variables, 85.7% of upper eyelid fold-related variables, and 40% of palpebral fissure-related variables), and LCAm (8.731°) had the highest TEM value. Only the rTEM of EnD and 14 variables (including EnD) of REM were <1% (41.7% of eyebrow-related variables and 26.7% of palpebral fissure-related variables; Figure 5). Thirteen variables of rTEM (37.5% of eyebrow-related variables and 26.7% of palpebral fissure-related variables) and 24 variables of REM (50% of brow-related variables, 42.9% of upper eyelid fold-related variables, and 60% of palpebral fissure-related variables) were between 1% and 3.9%, respectively; 13 rTEM (45.8% of brow-related variables and 13.3% of palpebral fissure-related variables) and five REM (37.5% of brow-related variables, 28.6% of upper eyelid fold-related variables, and 6.7% of palpebral fissure-related variables) variables were between 4% and 6.9%; four rTEM (12.5% of eyebrow-related variables and 28.6% of upper eyelid fold-related variables) and one REM (28.6% of upper eyelid fold-related variables) variables were between 7% and 10%. Nine rTEM (4.2% of brow-related variables, 100% of upper eyelid fold-related variables, and 6.7% [1/15] of palpebral fissure-related variables) and two REM values (28.6% [1/7] of upper eyelid fold-related variables and 6.7% of palpebral fissure-related variables) were >10%. The largest rTEM value was FPD (17.29%), while the largest REM value was LCAm (10.31%).

When the mean of two scans for each device was used for comparison, 39 variables had an ICC >0.75, and the remaining ten variables were between 0.4 and 0.75. Forty-four measurements had a MAD of <1 unit, and 35 measurements had a TEM of <1 unit. Four rTEM and 16 REM values were <1%, 14 rTEM and 21 REM values were between 1% and 3.9%, and 17 rTEM and 6 REM values were between 4% and 6.9%. Three rTEM and two REM values were between 7% and 10%, and eight rTEM and one REM values were >10%. Overall, applying the average of the two captures mildly improved inter-device reliability compared to using only the first capture.

4.5. DISCUSSION

We validated the reliability of portable devices in periocular applications for the first time using a periocular marker developed by Guo et al. (21). The mean results for the intra-device reliability metrics of MAD (0.13 and 0.12 units), REM (0.61% and 0.68%), TEM (1.02 and 0.80 units), rTEM (5.51% and 4.43%), and ICC (0.89 and 0.89) for devices M3 and H2 were highly comparable. For inter-device comparisons, the mean MAD, REM, TEM, rTEM, and ICC were 0.63 units, 2.83%, 1.31 units, 7.62%, and 0.79 units, respectively (0.62 units, 2.69%, 1.10 units, 5.57%, and 0.83 units if the mean values of H2 and M3 were used). Inter-device reliability decreased compared to intra-device reliability and all reliability metrics improved when quoting average values, indicating that we can reduce inter-device variation by using the average of the two captured images when the H2 device is used for photography.

Guo et al. first introduced 52 new periocular landmarks and validated the high reliability of the static VECTRA M3 stereophotogrammetric system for periocular anthropometry (21). The imaging system and landmarks were highly reliable for most measurements. Intra-rater measurements had the highest reliability, followed by inter-rater and intra-device measurements. The results of the M3 intra-device reliability analysis included MAD (0.98 units), REM (4.66%), TEM (0.96 units), rTEM (4.64%), and ICC (0.96). Our results were generally consistent with the aforementioned study, and some indicators were even more reliable.

Several recent studies have validated the reliability of portable stereophotogrammetric devices for facial imaging (5; 31). Camison et al. (5) verified that the portable VECTRA H1 and static 3dMD devices were highly comparable in facial imaging: 136 linear distances had an inter-device mean rTEM value of 1.13% (range, 0.44–2.48%). Fifty-five of these distances (40.4%) were in the "excellent" category (<1%), while the remaining 81 distances (59.6%) were in the "very good" range (<3.9%) (TEM, 0.84 mm). Gibelli et al. (31) and Kim et al. (34) compared the portable VECTRA H1 device with the static VECTRA M3 device in terms of the linear, angular, surface area, and volume measurement for reliability. The results, except for the lip and periocular regions, showed high repeatability for most linear, angular, and surface area measurements in M3 vs. M3, H1 vs. H1, and M3 vs. H1 comparisons (range, 82.2–98.7%; TEM, range, 0.3-2.0 mm, 0.4-1.8 degrees; rTEM, range, 0.2–3.1%). rTEM was primarily classified to provide excellent intra-device and good inter-device comparisons. Notably, they validated the results mainly for the non-periocular regions of the face, thus assessing significant differences in the linear distance and angular type of validation. The current results are generally less reliable

than previous studies, possibly due to the eye movements reported in the previous literature (35, 36). Furthermore, the measurements in the periocular region are all small, and previous studies have reported that reliability decreases as measurements decrease (37, 38).

Specifically, the highest reliability was found for most palpebral fissure-related variables in various comparisons, with rTEM primarily categorized as excellent, very good, or good within devices (M3 vs. M3: 0.26–6.39% and H2 vs. H2: 0.51–6.42%). Simultaneously, M3 and H2 comparisons were also excellent, very good, or good (0.02–5.34% and 0.66–6.20%) (first assessment and mean). The next most reliable assessment was for eyebrow-related variables, and within-device rTEM was mainly classified as very good or good (M3 vs. M3: 1.82–6.49% and H2 vs. H2: 1.33–6.02%), while M3 and H2 comparisons were also good (2.52–6.76% and 2.27–6.51%, respectively) (first evaluation and mean). The worst reliability was for the upper eyelid fold-related variables. Within-device rTEM was mainly classified as moderate or poor (M3 vs. M3: 9.88–13.87% and H2 vs. H2: 7.65–15.76%), while M3 compared to H1 (first evaluation and mean) had poor rTEM (11.15–17.29% and 12.15–15.61%, respectively).

TEM and rTEM values were generally consistent and reliable in their respective intra-device comparisons when using M3 and H2 scans for periocular data measurements. In contrast, TEM and rTEM values deteriorated in the M3 versus H2 comparison. This result may be due to the strong effect of involuntary head and eye movements during acquisition using the H2 device as it requires three consecutive images to be acquired, while the static M3 device acquires the same images simultaneously.

One limitation of the current study comes from the volunteers; only cooperative adults could be invited to participate because it is difficult to ensure that head, eye, and eyelid positions do not shift in children and non-cooperative individuals. Additionally, all data were collected at a fixed location, thus not fully reflecting the portability of the H2 device. Furthermore, the current study involved linear distance, curve, and angle measurements of the periocular region, without measuring its area and volume. Therefore, this study focused on comparing the differences in periocular measurements between healthy Caucasian adults on the two devices and did not include age, race, and patients in the study. Further studies should evaluate the device's reliability in different age groups, different ethnicities, bedside or other indoor settings for patients with limited mobility and the periocular area and volume measurement.

4.6. CONCLUSIONS

The intra-device reliability of the two categories of devices in this study was generally consistent, with a slightly poorer inter-device agreement. The palpebral fissure-related variables and eyebrow-related variables had good reliability both within and between devices. This validation study explored the measurement of linear distance, angle, and curve values in the periocular region with the new portable device VECTRA H2, making an essential contribution to validating the VECTRA H2 device in the periocular region. Previous studies used the earlier generation of portable devices, VECTRA H1, and mainly verified the reliability in non-ocular locations of the face. Compared to static devices, portable instruments are relatively inexpensive and location-independent, allowing photography for patients with limited mobility or in remote areas. However, it is disadvantageous in that it has slightly lower reliability than static devices. Therefore, we need to select the most suitable instrument for future clinical applications according to what the actual situation presents.

4.7. DECLARATIONS

DATA AVAILABILITY STATEMENT

The original contributions presented in the study are included in the article/supplementary material, further inquiries can be directed to the corresponding authors.

ETHICS STATEMENT

The studies involving human participants were reviewed and approved by the Ethics Committee of Cologne University. The patients/participants provided their written informed consent to participate in this study. Written informed consent was obtained from the individual(s) for the publication of any potentially identifiable images or data included in this article.

AUTHOR CONTRIBUTIONS

WF, AR, and LH: conception, design, and provision of study materials and participants. LH: administrative support. All authors: collection and assembly of data, data analysis and interpretation, and manuscript writing. All authors contributed to the article and approved the submitted version.

FUNDING

This study was supported by State Scholarship Fund from the China Scholarship Council (No. 202008080258).

ACKNOWLEDGMENTS

The authors thank Editage (www.editage.com) for English language editing. The authors also thank Canfield Scientific GmbH, Bielefeld, Germany for providing the H2 free of charge.

4.8. REFERENCES

1. Verhulst A, Hol M, Vreeken R, Becking A, Ulrich D, Maal T. Three-Dimensional Imaging of the Face: A Comparison Between Three Different Imaging Modalities. Aesthetic Surgery Journal. 2018;38(6):579-85.

2. Choi JW, Lee JY, Oh T-S, Kwon SM, Yang SJ, Koh KS. Frontal soft tissue analysis using a 3 dimensional camera following two-jaw rotational orthognathic surgery in skeletal class III patients. Journal of Cranio-Maxillofacial Surgery. 2014;42(3):220-6.

3. Jung J, Lee CH, Lee JW, Choi BJ. Three dimensional evaluation of soft tissue after orthognathic surgery. Head Face Med. 2018;14(1):21.

4. Terzic A, Schouman T, Scolozzi PJRds, de chirurgie maxillo-faciale et de chirurgie orale. Accuracy of morphological simulation for orthognatic surgery. Assessment of a 3D image fusion software. 2013;114(4):276-82.

5. Camison L, Bykowski M, Lee WW, Carlson JC, Roosenboom J, Goldstein JA, et al. Validation of the Vectra H1 portable three-dimensional photogrammetry system for facial imaging. International journal of oral and maxillofacial surgery. 2018;47(3):403-10.

6. Meier JD, Glasgold RA, Glasgold MJ. 3D photography in the objective analysis of volume augmentation including fat augmentation and dermal fillers. Facial plastic surgery clinics of North America. 2011;19(4):725-35, ix.

7. Miller TR. Long-term 3-Dimensional Volume Assessment After Fat Repositioning Lower Blepharoplasty. JAMA facial plastic surgery. 2016;18(2):108-13.

8. Jacono AA, Bryant LM, Ahmedli NN. A Novel Extended Deep Plane Facelift Technique for Jawline Rejuvenation and Volumization. Aesthet Surg J. 2019;39(12):1265-81.

9. Kunjur J, Sabesan T, Ilankovan V. Anthropometric analysis of eyebrows and eyelids: an inter-racial study. Br J Oral Maxillofac Surg. 2006;44(2):89-93.

10. Liu Y, Kau CH, Pan F, Zhou H, Zhang Q, Zacharopoulos GV. A 3-dimensional anthropometric evaluation of facial morphology among Chinese and Greek population. The Journal of craniofacial surgery. 2013;24(4):e353-8.

11. Erbagci I, Erbagci H, Kizilkan N, Gumusburun E, Bekir N. The effect of age and gender on the anatomic structure of Caucasian healthy eyelids. Saudi Med J. 2005;26(10):1535-8.

12. Sforza C, Grandi G, Catti F, Tommasi DG, Ugolini A, Ferrario VF. Age- and sex-related changes in the soft tissues of the orbital region. Forensic Sci Int. 2009;185(1-3):115.e1-8.

13. Cartwright MJ, Kurumety UR, Nelson CC, Frueh BR, Musch DC. Measurements of upper eyelid and eyebrow dimensions in healthy white individuals. Am J Ophthalmol. 1994;117(2):231-4.

14. Metzler P, Sun Y, Zemann W, Bartella A, Lehner M, Obwegeser JA, et al. Validity of the 3D VECTRA photogrammetric surface imaging system for cranio-maxillofacial anthropometric measurements. Oral and Maxillofacial Surgery. 2014;18(3):297-304.

15. Dindaroğlu F, Kutlu P, Duran GS, Görgülü S, Aslan E. Accuracy and reliability of 3D stereophotogrammetry: A comparison to direct anthropometry and 2D photogrammetry. The Angle Orthodontist. 2016;86(3):487-94.

16. Modabber A, Peters F, Kniha K, Goloborodko E, Ghassemi A, Lethaus B, et al. Evaluation of the accuracy of a mobile and a stationary system for three-dimensional facial scanning. J Cranio Maxillofacial Surg. (2016) 44:1719–24. doi: 10.1016/j.jcms.2016.08.008

17. Guo Y, Schaub F, Mor JM, Jia R, Koch KR, Heindl LM. A Simple Standardized Three-Dimensional Anthropometry for the Periocular Region in a European Population. Plast Reconstr Surg. 2020;145(3):514e-23e.

18. Guo Y, Rokohl AC, Lin M, Heindl LM. Three-dimensional anthropometry in periorbital region. Annals of Eye Science. 2020;6:8.

19. Hou X, Rokohl AC, Meinke MM, Li S, Liu J, Fan W, et al. A novel standardized distraction test to evaluate lower eyelid tension using three-dimensional stereophotogrammetry. Quantitative Imaging in Medicine and Surgery. 2021;11(8):3735-48.

20. Hou X, Rokohl AC, Meinke MM, Liu J, Li S, Fan W, et al. Standardized Three-Dimensional Lateral Distraction Test: Its Reliability to Assess Medial Canthal Tendon Laxity. Aesthetic Plast Surg. 2021.

21. Guo Y, Rokohl AC, Schaub F, Hou X, Liu J, Ruan Y, et al. Reliability of periocular anthropometry using three-dimensional digital stereophotogrammetry. Graefes Arch Clin Exp Ophthalmol. 2019;257(11):2517-31.

22. Guo Y, Hou X, Rokohl AC, Jia R, Heindl LM. Reliability of Periocular Anthropometry: A Comparison of Direct, 2-Dimensional, and 3-Dimensional Techniques. Dermatol Surg. 2020;46(9):e23-e31.

23. Guo Y, Liu J, Ruan Y, Rokohl AC, Hou X, Li S, et al. A novel approach quantifying the periorbital morphology: A comparison of direct, 2-dimensional, and 3-dimensional technologies. J Plast Reconstr Aesthet Surg. 2021;74(8):1888-99.

24. Liu J, Guo Y, Arakelyan M, Rokohl AC, Heindl LM. Accuracy of Areal Measurement in the Periocular Region Using Stereophotogrammetry. J Oral Maxillofac Surg. 2021;79(5):1106.e1-.e9.

25. Liu J, Rokohl AC, Guo Y, Li S, Hou X, Fan W, et al. Reliability of Stereophotogrammetry for Area Measurement in the Periocular Region. Aesthetic Plast Surg. 2021;45(4):1601-10.

26. Tzou C-HJ, Artner NM, Pona I, Hold A, Placheta E, Kropatsch WG, et al. Comparison of three-dimensional surface-imaging systems. Journal of Plastic, Reconstructive & Aesthetic Surgery. 2014;67(4):489-97.

27. Birgfeld CB, Saltzman BS, Luquetti DV, Latham K, Starr JR, Heike CL. Comparison of two-dimensional and three-dimensional images for phenotypic assessment of craniofacial microsomia. The Cleft palate-craniofacial journal : official publication of the American Cleft Palate-Craniofacial Association. 2013;50(3):305-14.

28. Naudi KB, Benramadan R, Brocklebank L, Ju X, Khambay B, Ayoub A. The virtual human face: superimposing the simultaneously captured 3D photorealistic skin surface of the face on the untextured skin image of the CBCT scan. Int J Oral Maxillofac Surg. 2013;42(3):393-400.

29. Yamamoto S, Miyachi H, Fujii H, Ochiai S, Watanabe S, Shimozato K. Intuitive facial imaging method for evaluation of postoperative swelling: a combination of 3-dimensional computed tomography and laser

surface scanning in orthognathic surgery. J Oral Maxillofac Surg. (2016) 74:2506.e1–10. doi: 10.1016/j.joms.2016.08.039

30. Knoops PG, Beaumont CA, Borghi A, Rodriguez-Florez N, Breakey RW, Rodgers W, et al. Comparison of three-dimensional scanner systems for craniomaxillofacial imaging. J Plast Reconstr Aesthet Surg. (2017) 70:441–9. doi: 10.1016/j.bjps.2016.12.015

31. Gibelli D, Pucciarelli V, Cappella A, Dolci C, Sforza C. Are Portable Stereophotogrammetric Devices Reliable in Facial Imaging? A Validation Study of VECTRA H1 Device. J Oral Maxillofac Surg. 2018;76(8):1772-84.

32. Ulijaszek SJ, Kerr DA. Anthropometric measurement error and the assessment of nutritional status. Br J Nutr. 1999;82(3):165-77.

33. Andrade LM, Rodrigues da Silva AMB, Magri LV, Rodrigues da Silva MAM. Repeatability Study of Angular and Linear Measurements on Facial Morphology Analysis by Means of Stereophotogrammetry. The Journal of craniofacial surgery. 2017;28(4):1107-11.

34. Kim AJ, Gu D, Chandiramani R, Linjawi I, Deutsch ICK, Allareddy V, et al. Accuracy and reliability of digital craniofacial measurements using a small-format, handheld 3D camera. Orthod Craniofac Res. 2018.

35. de Menezes M, Rosati R, Allievi C, Sforza C. A photographic system for the three-dimensional study of facial morphology. Angle Orthod. 2009;79(6):1070-7.

36. Ferrario VF, Sforza C, Poggio CE, Cova M, Tartaglia G. Preliminary evaluation of an electromagnetic three-dimensional digitizer in facial anthropometry. The Cleft palate-craniofacial journal : official publication of the American Cleft Palate-Craniofacial Association. 1998;35(1):9-15.

37. Jamison PL, Ward RE. Brief communication: measurement size, precision, and reliability in craniofacial anthropometry: bigger is better. Am J Phys Anthropol. 1993;90(4):495-500.

38. Ward RE, Jamison PL. Measurement precision and reliability in craniofacial anthropometry: implications and suggestions for clinical applications. J Craniofac Genet Dev Biol. 1991;11(3):156-64.

4.9. APPENDIX

4.9.1. Figure Legends

Figure 1. The process of 3D image acquisition with Vectra H2 portable camera

The volunteer follows the instructions to turn the head to the left (A), turn the head to look forward (B), and finally turn the head to the right (C). The application instruction screen for each step is displayed in the upper right corner.

Figure 2. Description of periocular anthropometric landmarks used in this study

Periocular anthropometry was performed according to Guo et al.[58]

Figure 3. Intra- and inter-device of intraclass correlation coefficient (ICC) for all periocular region measurements of 3D images.

ICC values allowed the classification of the agreement into three classes: <0.4, poor agreement; 0.4–0.75, satisfactory; and $\geqslant$0.75, excellent.

Figure 4. Intra- and inter-device mean absolute difference (MAD) and technical error of measurement (TEM) for periocular measurements on all 3D images

The acceptable error threshold is set to 1 unit.

Figure 5. Intra- and inter-device relative error of measurement (REM) for all periocular region measurements of 3D images

Reliability category criteria were as follows: excellent, <1%; very good, 1–3.9%; good, 4–6.9%; moderate, 7–9.9%; and poor, >10%.

Figure 6. Intra- and inter-device of relative technical error of measurement (rTEM) for all periocular region measurements of 3D images

Reliability category criteria were as follows: excellent, <1%; very good, 1–3.9%; good, 4–6.9%; moderate, 7–9.9%; and poor, >10%.

Figure 1. The process of 3D image acquisition with Vectra H2 portable camera

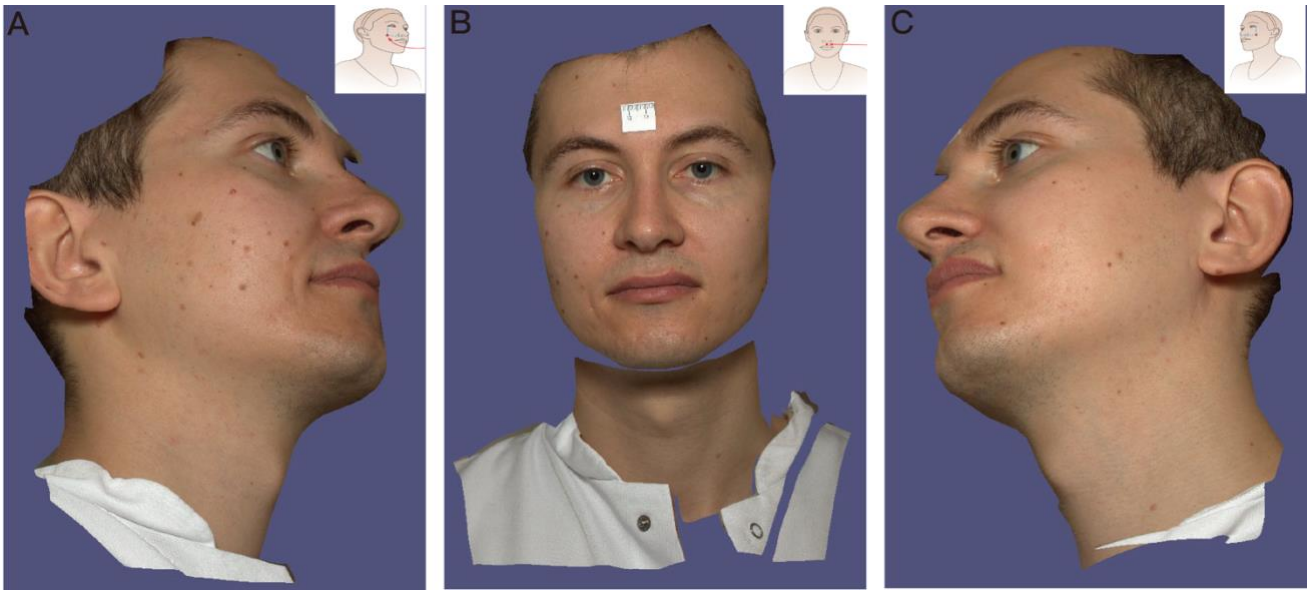

Figure 2. Description of periocular anthropometric landmarks used in this study

Periocular anthropometry was performed according to Guo et al.[58]

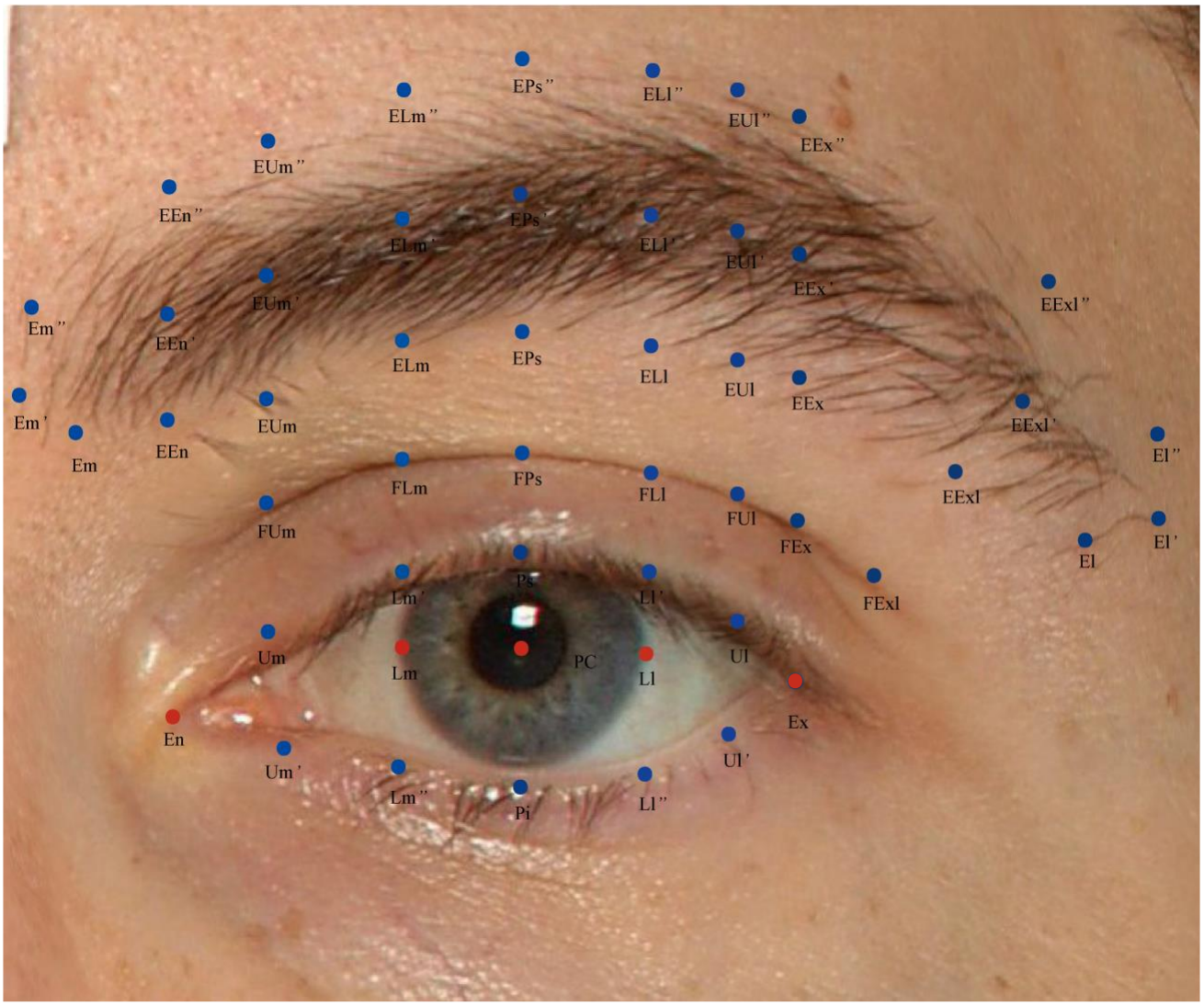

Figure 3. Intra- and inter-device of intraclass correlation coefficient (ICC) for all periocular region measurements of 3D images.

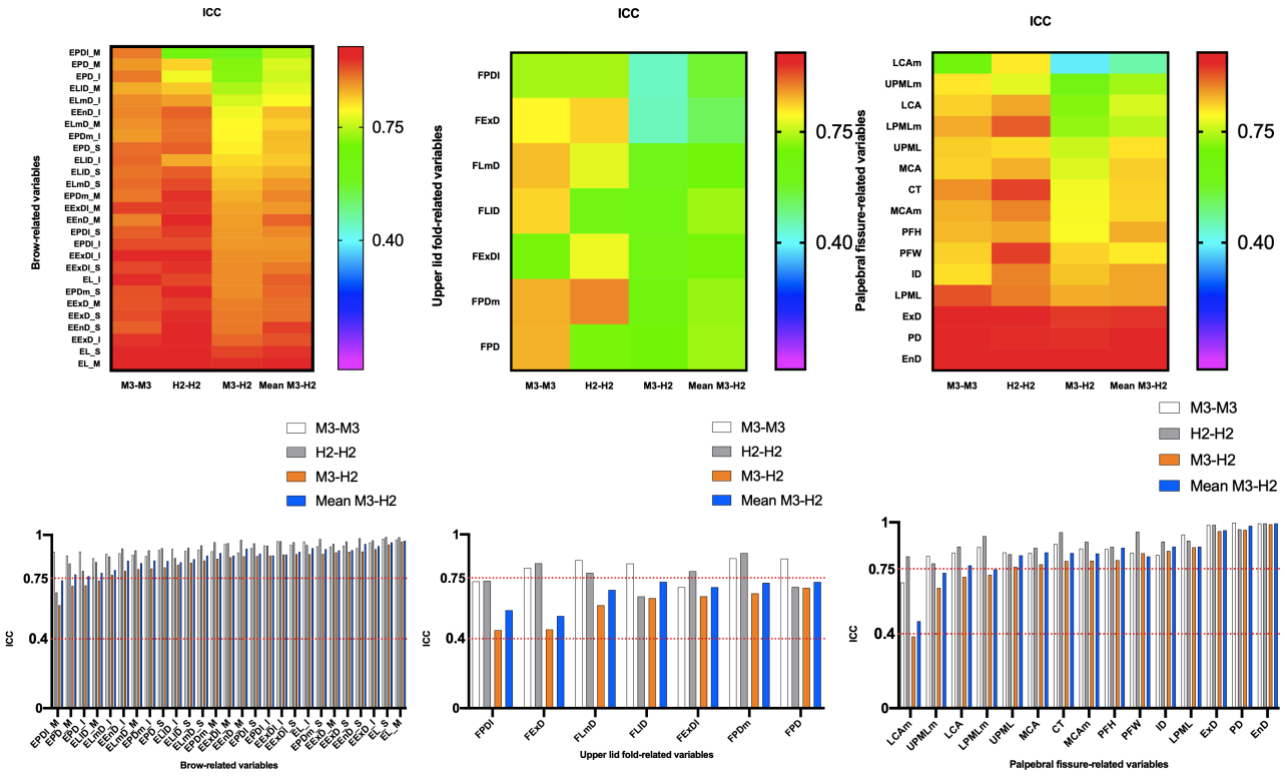

Figure 4. Intra- and inter-device mean absolute difference (MAD) and technical error of measurement (TEM) for periocular measurements on all 3D images

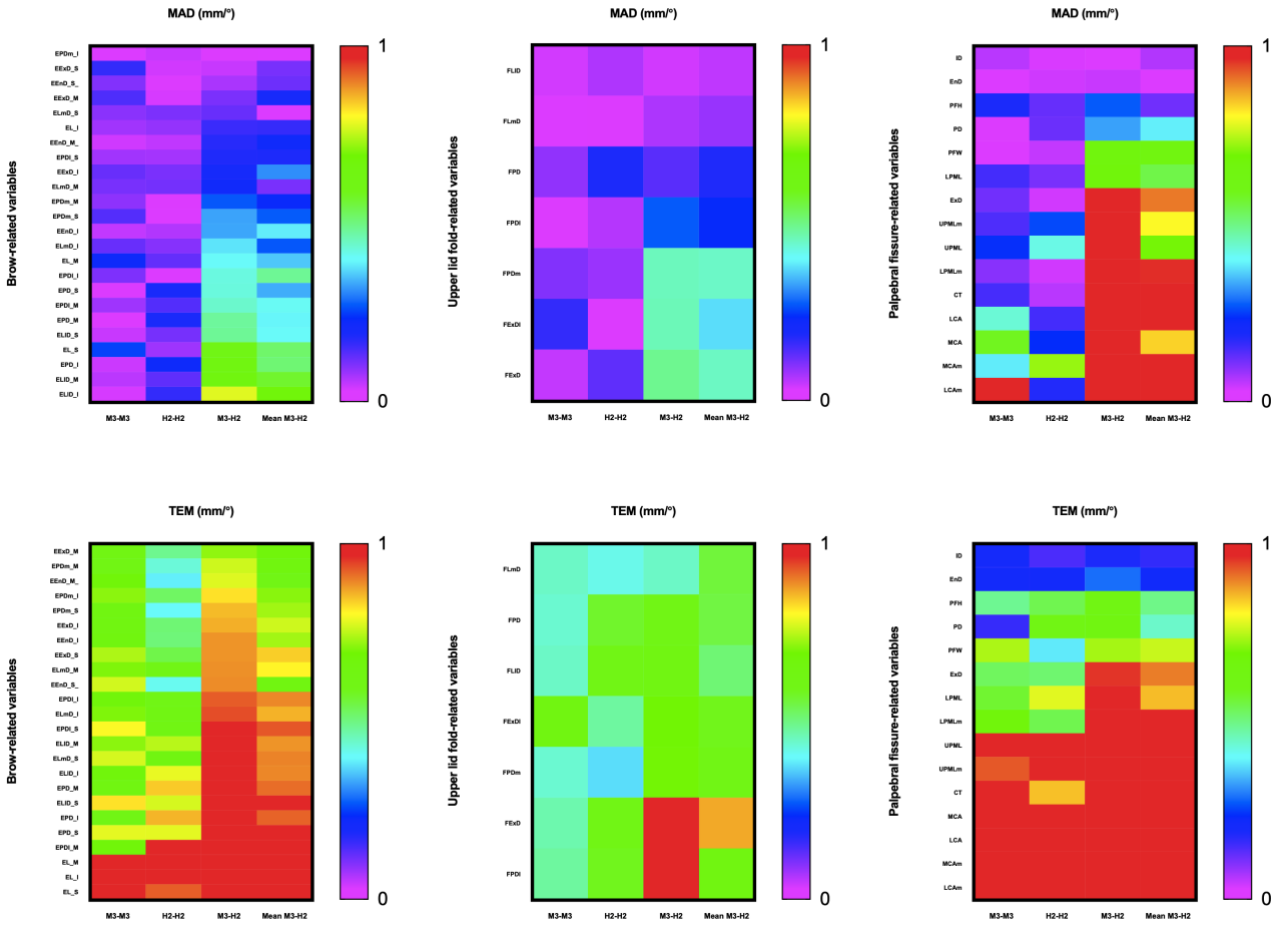

Figure 5. Intra- and inter-device relative error of measurement (REM) for all periocular region measurements of 3D images

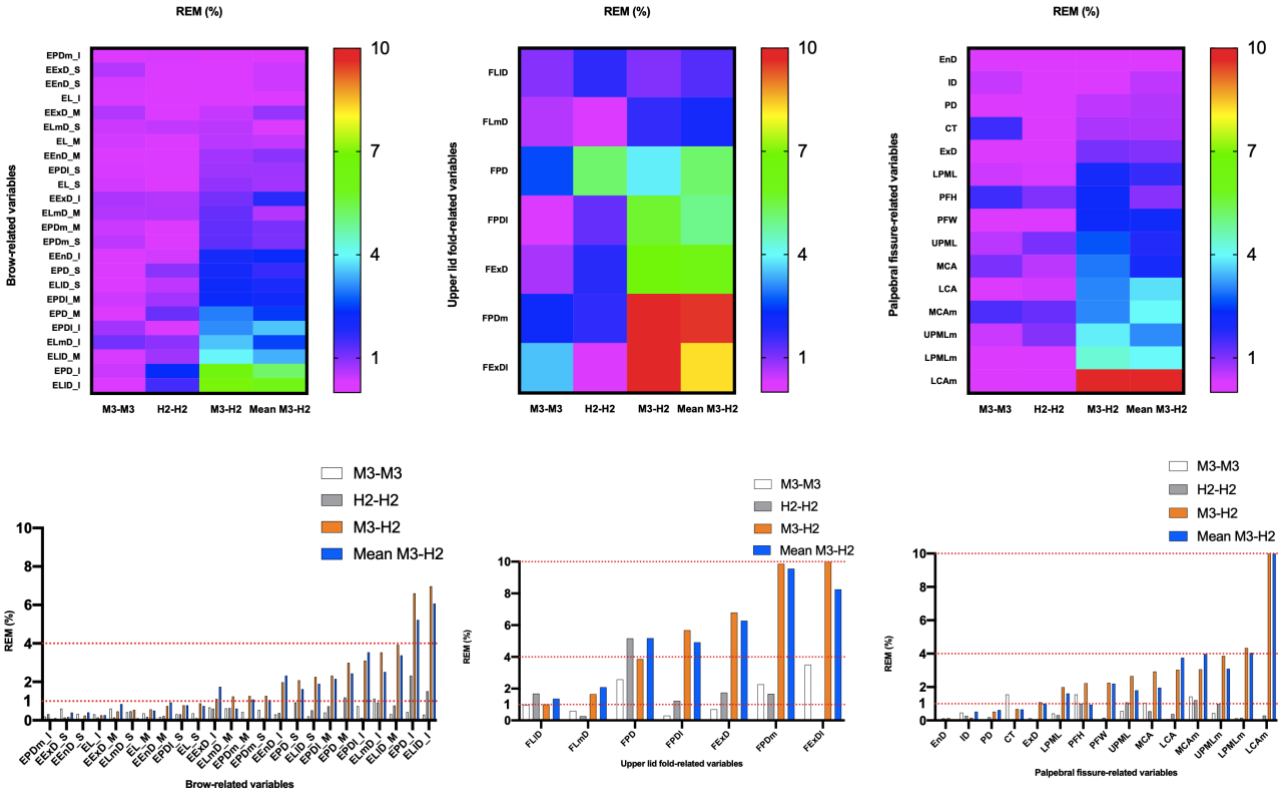

Figure 6. Intra- and inter-device of relative technical error of measurement (rTEM) for all periocular region measurements of 3D images

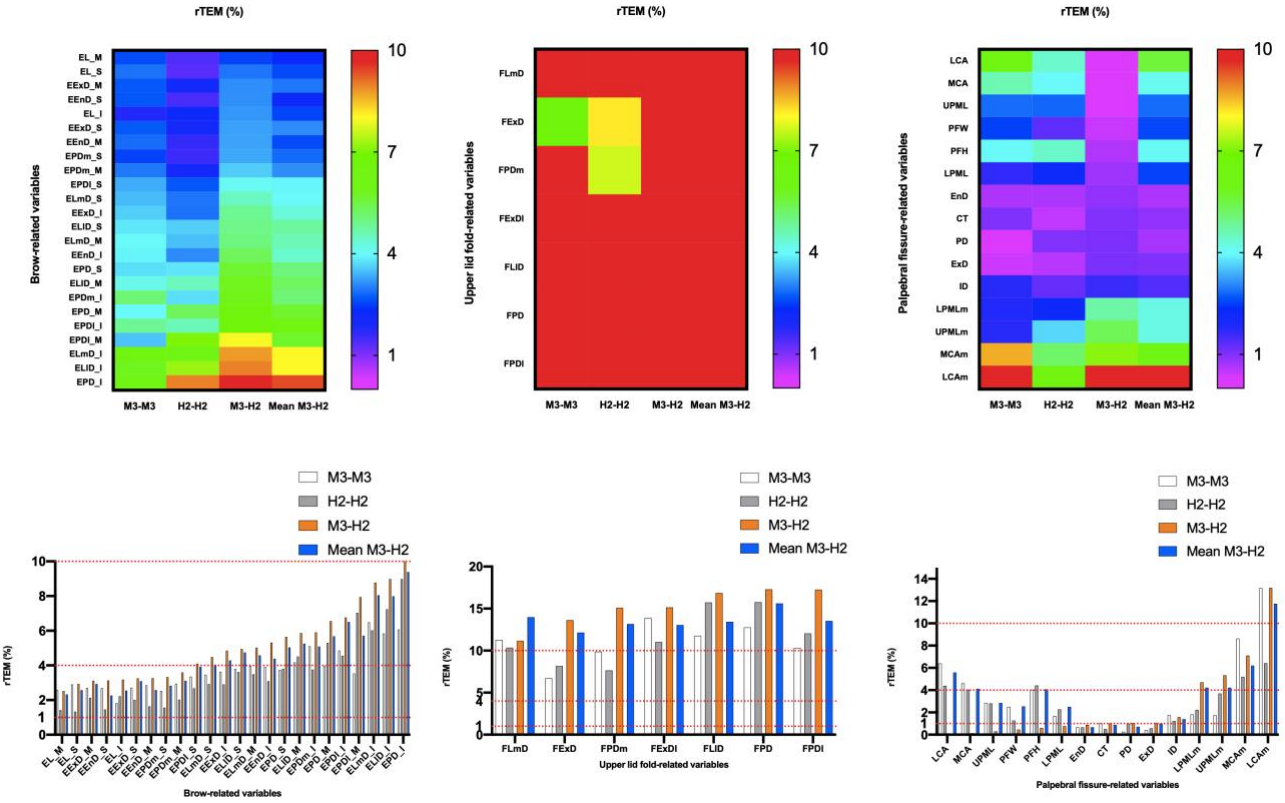

4.9.2. TABLES

Table Legends

Table 1:

Definition of abbreviations for periocular landmarks, modified from Guo et al.[58]

Table 2:

List of linear distance, curve, and angle measurement variables for the periocular region, derived from Guo et al.[58]

Table 3:

Means and standard deviations (SDs) of all measurements (mm or degrees)

Table 4:

Intra-device reliability results of VECTRA M3 and H2 for periocular measurements

Table 5:

Inter-device reliability results of VECTRA M3 and H2 for periocular measurements

Table 6:

Percentage of different periocular measurement variables in each reliability rating classification for VECTRA M3 and H2

Table 1. Definition of abbreviations for periocular landmarks, modified from Guo et al.[58]

Abbreviation of Landmarkers	Definition
En	Endocanthion, inner commissure of the palpebral fissure
Ex	Exocanthion, outer commissure of the lower and upper eyelash roots of the palpebral fissure
Pc	Pupillary center
Lm	Medial corneoscleral limbus point horizontal to pupillary center
Ll	Lateral corneoscleral limbus point horizontal to pupillary center
Em	Inferior margin point of the medial eyebrow end (sometimes locates at the same place with EEn);
Em"	superior margin point
Em'	middle point
EEn	Inferior margin point of eyebrow vertical to En
EEn"	Superior margin point of eyebrow vertical to En
EEn'	Middle point of eyebrow vertical to En
Um	Middle point between En and Lm'at the upper palpebral margin on the lash roots

Um'	Middle point between En and Lm" at the lower palpebral margin on the lash roots
FUm	Point vertical to Um at the lid fold superioris
EUm	Point vertical to Um at the inferior margin of eyebrows
EUm"	Point vertical to Um at the superior margin point
EUm'	Point vertical to Um at the middle point
Lm'	Point vertical to Lm at the upper palpebral margin on the lash roots
Lm"	Point vertical to Lm at the lower palpebral margin on the lash roots
FLm	Point vertical to Lm at the lid fold superioris
ELm	Point vertical to Lm at the inferior margin of eyebrows
ELm"	Point vertical to Lm at the superior margin of eyebrows
ELm'	Point vertical to Lm at the middle margin of eyebrows
Ps	Palpebrale superioris, Point vertical to Pc at the upper palpebral margin on the lash roots
Pi	Palpebrale inferioris, Point vertical to Pc at the lower palpebral margin on the lash roots
FPs	Point vertical to Pc at the lid fold superioris
EPs	Point vertical to Pc at the inferior margin of eyebrows

EPs"	Point vertical to Pc at the superior margin of eyebrows
EPs'	Point vertical to Pc at the middle margin of eyebrows
LI'	Point vertical to LI at the upper palpebral margin on the lash roots
LI"	Point vertical to LI at the lower palpebral margin on the lash roots
FLI	Point vertical to LI at the lid fold superioris
ELI	Point vertical to LI at the inferior margin of eyebrows
ELI"	Point vertical to LI at the superior margin of eyebrows
ELI'	Point vertical to LI at the middle margin of eyebrows
UI	The middle between Ex and LI'at the upper palpebral margin on the lash roots
UI'	The middle between Ex and LI"at the lower palpebral margin on the lash roots
FUI	FUI Point vertical to UI at the lid fold superioris
EUI	Point vertical to UI at the inferior margin of eyebrows
EUI"	Point vertical to UI at the superior margin of eyebrows
EUI'	Point vertical to UI at the middle margin of eyebrows
FEx	Point vertical to Ex at the lid fold superioris

EEx	Point vertical to Ex at the inferior margin of eyebrows
EEx”	Point vertical to Ex at the superior margin of eyebrows
EEx’	Point vertical to Ex at the middle margin of eyebrows
FExl	Point vertical to Ex at the lid fold superioris in lateral view
EExl	Point vertical to Ex at the inferior margin of eyebrows in lateral view
EExl”	Point vertical to Ex at the superior margin of eyebrows in lateral view
EExl’	Point vertical to Ex at the middle margin of eyebrows in lateral view
El	inferior margin of the lateral eyebrow end
El”	superior margin of the lateral eyebrow end
El’	middle margin of the lateral eyebrow end

Table 2. List of linear distance, curve, and angle measurement variables for the periocular region, derived from Guo et al.[58]

Abbreviation	Definition	Landmarks
Liner distances		
PFW	Palpebral fissure width	En-Ex
PFH	Palpebral fissure height	Ps-Pi
EEnD_I	Eyebrow-endocanthion distance of the inferior point	EEn-En
EEnD_M_	Eyebrow-endocanthion distance of the middle point	EEn'-En
EEnD_S_	Eyebrow-endocanthion distance of the inferior, middle, or superior point	EEn"-En
FPDm	Upper lid fold-palpebral margin distance (medial)	FUm-Um
EPDm_I	Eyebrow-palpebral margin distance (medial) of the inferior point	EUm-Um
EPDm_M	Eyebrow-palpebral margin distance (medial) of the middle point	EUm'-Um
EPDm_S	Eyebrow-palpebral margin distance	EUm"-Um

	(medial) of the superior point	
FLmD	Upper lid fold-palpebral margin distance (medial limbus)	FLm-Lm'
ELmD_I	Eyebrow-palpebral margin distance (medial limbus) of the inferior point	ELm-Lm'
ELmD_M	Eyebrow-palpebral margin distance (medial limbus) of the middle point	ELm'-Lm'
ELmD_S	Eyebrow-palpebral margin distance (medial limbus) of the superior point	ELm"-Lm'
FPD	Upper lid fold-palpebral margin distance, similar to upper lid fold height	Ps-FPs
EPD_I	Eyebrow-palpebral margin (Ps) distance of the inferior (similar to upper lid height) point	Ps-EPs
EPD_M	Eyebrow-palpebral margin (Ps) distance of the middle point	Ps-EPs'
EPD_S	Eyebrow-palpebral margin (Ps) distance of the superior point	Ps-EPs"
FLID	Upper lid fold-palpebral margin	FLI-LI'

	distance (lateral limbus)	
ELID_I	Eyebrow-palpebral margin distance (lateral limbus) of the inferior point	ELI-LI'
ELID_M	Eyebrow-palpebral margin distance (lateral limbus) of the middle point	ELI'-LI'
ELID_S	Eyebrow-palpebral margin distance (lateral limbus) of the superior point	ELI"-LI'
FPDl	Upper lid fold-palpebral margin distance (lateral)	FUI-UI
EPDl_I	Eyebrow-palpebral margin distance (lateral) of the inferior point	EUI-UI
EPDl_M	Eyebrow-palpebral margin distance (lateral) of the middle point	EUI'-UI
EPDl_S	Eyebrow-palpebral margin distance (lateral) of the superior point	EUI"-UI
FExD	Upper lid fold-exocanthion distance	FEx-Ex

EExD_I	Eyebrow-exocanthion distance of the inferior point	EEx-Ex
EExD_M	Eyebrow-exocanthion distance of the middle point	EEx'-Ex
EExD_S	Eyebrow-exocanthion distance of the superior point	EEx"-Ex
FExDl	Upper lid fold-exocanthion distance (lateral)	FExl-Ex
EExDl_I	Eyebrow-exocanthion distance (lateral) of the inferior point	EExl-Ex
EExDl_M	Eyebrow-exocanthion distance (lateral) of the middle point	EExl'-Ex
EExDl_S	Eyebrow-exocanthion distance (lateral) of the superior point	EExl"-Ex
ID	Iris diameter	Lm-Ll
EnD	Inner intercanthal distance	En (left)-En (right)
PD	Interpupillary distance	Pc (left)-Pc (right)
ExD	Outer intercanthal distance	Ex (left)-Ex (right)

Curvatures		
UPML	Upper palpebral margin length	En-Um-Lm'-Ps-Ll'-Ul-Ex
UPMLm	Upper palpebral margin length (more points)	Including 4 more midpoints between Lm'-Ps-Ll'-Ul-Ex
LPML	Lower palpebral margin length	En-Um'-Lm"-Pi-Ll"-Ul'-Ex
LPMLm	Lower palpebral margin length (more points)	Including 4 more midpoints between Lm"-Pi-Ll"-Ul'-Ex
EL_I	Inferior eyebrow length	Em-EEn-EUm-ELm-EPs-ELl-EUl-EEx-EExl-El
EL_M	Middle eyebrow length	Em'-EEn'-EUm'-ELm'-EPs'-ELl'-EUl'-EEx'-EExl'-El'
EL_S	Superior eyebrow length	Em"-EEn"-EUm"-ELm"-EPs"-ELl"-EUl"-EEx"-EExl"-El"
Angles		
MCA	Medial canthal angle	Ps-En-Pi
MCAm	Medial canthal angle (medial)	Um-En-Um'
LCA	Lateral canthal angle	Ps-Ex-Pi
LCAm	Lateral canthal angle (medial)	Ul-Ex-Ul'

CT	Canthal tilt	Ex (left)-En (left)-En (right), or Ex (right)-En (right)-En (left)

Table 3. Means and standard deviations (SDs) of all measurements (mm or degrees)

Parameters	M3				H2			
	Capture 1		Capture 2		Capture 1		Capture 2	
	Mean	SD	Mean	SD	Mean	SD	Mean	SD
Liner distances(mm)								
PFW	29.38	1.76	29.37	1.86	30.05	1.69	30.00	1.68
PFH	12.01	1.28	12.19	1.26	12.28	1.46	12.15	1.49
EEnD_I	16.78	1.95	16.84	2.07	16.46	1.87	16.39	1.72
EEnD_M_	23.81	2.11	23.84	2.11	23.63	2.26	23.58	2.25
EEnD_S_	28.45	2.81	28.55	2.71	28.38	2.91	28.38	2.93
FPDm	4.37	1.16	4.47	1.17	4.83	1.12	4.91	1.13
EPDm_I	13.93	1.95	13.96	2.11	13.94	1.77	13.98	1.71
EPDm_M	21.05	1.97	21.14	2.04	21.32	2.11	21.33	2.09
EPDm_S	25.50	2.49	25.64	2.52	25.83	2.62	25.85	2.59
FLmD	3.96	1.14	3.93	1.16	4.02	0.86	4.04	0.91
ELmD_I	10.88	2.04	10.76	2.17	10.50	1.81	10.60	1.77

ELmD_M	17.75	1.96	17.64	2.15	17.53	2.00	17.65	2.08
ELmD_S	22.23	2.56	22.13	2.69	22.10	2.58	22.21	2.66
FPD	3.39	1.16	3.48	1.18	3.52	0.97	3.71	1.08
EPD_I	10.08	2.01	10.03	1.92	9.43	1.91	9.66	1.83
EPD_M	16.26	1.82	16.28	1.88	15.78	1.98	15.97	2.13
EPD_S	20.83	2.57	20.83	2.70	20.40	2.74	20.59	2.86
FLID	3.77	1.08	3.80	1.08	3.81	1.02	3.87	0.99
ELID_I	11.54	2.43	11.50	2.28	10.76	2.23	10.92	2.04
ELID_M	17.11	1.90	17.06	1.97	16.45	1.80	16.58	1.95
ELID_S	21.68	2.57	21.63	2.82	21.19	2.71	21.30	2.90
FPDl	4.62	0.94	4.63	0.89	4.89	1.20	4.83	1.04
EPDl_I	13.90	2.78	14.01	2.68	13.48	2.51	13.46	2.38
EPDl_M	19.24	2.14	19.32	2.19	18.80	2.53	18.94	2.03
EPDl_S	23.75	2.78	23.83	2.99	23.57	2.75	23.64	2.94
FExD	6.93	1.05	6.89	1.06	7.42	1.47	7.29	1.47
EExD_I	17.88	3.09	18.01	3.11	17.69	2.91	17.58	2.89
EExD_M	23.07	2.35	23.21	2.44	22.96	2.14	22.93	2.14

EExD_S	27.13	2.92	27.30	2.97	27.09	2.71	27.13	2.79
FExDl	4.77	1.17	4.61	1.18	4.31	1.04	4.32	1.02
EExDl_I	14.77	3.21	14.73	3.21	13.65	3.13	13.49	3.03
EExDl_M	19.44	2.58	19.42	2.57	18.60	2.42	18.50	2.38
EExDl_S	23.38	3.19	23.43	3.13	22.71	3.03	22.63	3.04
ID	11.91	0.49	11.97	0.49	11.90	0.46	11.86	0.44
EnD*	32.45	2.60	32.43	2.71	32.40	2.72	32.44	2.75
PD*	62.71	3.24	62.72	3.26	62.39	3.14	62.27	3.19
ExD*	89.93	4.29	90.04	4.22	90.91	4.28	90.87	4.27
Curvatures (mm)								
UPML	38.01	2.75	38.25	2.62	39.03	2.64	38.61	2.55
UPMLm	25.32	2.22	25.46	2.12	26.32	2.18	26.06	1.89
LPML	33.60	2.34	33.75	2.20	34.28	2.41	34.17	2.52
LPMLm	23.20	1.95	23.30	1.71	24.23	1.97	24.19	1.97
EL_I	59.14	5.63	59.22	5.43	59.30	5.64	59.39	5.30
EL_M	70.96	9.28	71.19	9.17	71.37	8.74	71.49	8.55

EL_S	68.91	8.86	69.16	8.84	69.52	8.35	69.59	8.31
Angles (°)								
MCA	41.79	4.45	42.38	4.07	43.04	4.52	42.80	4.78
MCAm	61.65	9.36	62.03	8.71	59.79	9.40	59.07	9.54
LCA	40.93	4.66	41.36	4.63	39.70	4.79	39.55	4.78
LCAm	69.64	10.56	70.65	10.59	62.82	9.44	62.64	9.30
CT	168.33	3.53	168.18	3.44	167.19	3.62	167.13	3.67

*N = 60; for the rest, N = 120; SD, standard deviations

Table 4. Intra-device reliability results of VECTRA M3 and H2 for periocular measurements

Device	**M3 vs M3**						**H2 vs H2**					
Comparison	**ICC (CI 95%)**	**MAD**	**TEM**	**rTEM**	**REM**	**p value**	**ICC**	**MAD**	**TEM**	**rTEM**	**REM**	**p value**
Liner distances(mm)												
PFW	0.84 (0.77-0.88)	0.02	0.74	2.51	0.06	0.948	0.95 (0.93-0.96)	0.05	0.38	1.27	0.16	0.332
PFH	0.86 (0.79-0.90)	0.19	0.49	4.03	1.56	**<0.001** †	0.87 (0.82-0.91)	0.12	0.54	4.42	1.01	0.078
EEnD_I	0.89	0.05	0.66	3.91	0.31	0.544	0.92	0.06	0.51	3.09	0.38	0.349

	(0.85-0.93)						(0.89-0.94)					
EEnD_M_	0.90 (0.86-0.93)	0.04	0.68	2.85	0.16	0.665	0.97 (0.96-0.98)	0.05	0.39	1.64	0.22	0.305
EEnD_S_	0.92 (0.89-0.95)	0.10	0.77	2.68	0.34	0.331	0.98 (0.97-0.99)	0.00	0.41	1.45	0.00	0.996
FPDm	0.86 (0.81-0.90)	0.10	0.44	9.88	2.27	0.075	0.89 (0.85-0.92)	0.08	0.37	7.65	1.67	0.062 †
EPDm_I	0.88 (0.83-0.91)	0.03	0.71	5.11	0.20	0.765	0.91 (0.87-0.94)	0.05	0.52	3.75	0.32	0.508
EPDm_M	0.91 (0.87-0.93)	0.09	0.62	2.94	0.43	0.259	0.96 (0.94-0.97)	0.01	0.43	2.02	0.06	0.848

EPDm_S	0.93 (0.91-0.95)	0.14	0.65	2.53	0.54	0.100	0.98 (0.97-0.98)	0.03	0.40	1.56	0.10	0.622
FLmD	0.85 (0.79-0.89)	0.02	0.45	11.28	0.60	0.681	0.78 (0.70-0.84)	0.01	0.42	10.34	0.27	0.860
ELmD_I	0.89 (0.85-0.92)	0.12	0.70	6.49	1.12	0.183	0.88 (0.83-0.91)	0.10	0.64	6.02	0.92	0.237
ELmD_M	0.89 (0.84-0.92)	0.11	0.70	3.97	0.62	0.228	0.91 (0.87-0.94)	0.11	0.61	3.49	0.64	0.160
ELmD_S	0.92 (0.88-0.94)	0.09	0.77	3.47	0.42	0.540 †	0.94 (0.92-0.96)	0.11	0.65	2.92	0.47	0.211
FPD	0.86	0.09	0.44	12.76	2.58	0.091 †	0.70	0.19	0.57	15.76	5.16	0.110

	(0.81-0.90)						(0.59-0.78)					
EPD_I	0.90 (0.87-0.93)	0.04	0.61	6.07	0.43	0.586	0.79 (0.71-0.85)	0.22	0.86	8.98	2.32	**0.044**
EPD_M	0.88 (0.83-0.92)	0.02	0.64	3.95	0.10	0.854	0.84 (0.77-0.88)	0.19	0.84	5.30	1.19	0.810
EPD_S	0.91 (0.88-0.94)	0.01	0.78	3.75	0.03	0.956	0.92 (0.89-0.95)	0.19	0.78	3.81	0.93	0.057
FLID	0.83 (0.77-0.88)	0.04	0.45	11.76	0.97	0.242 †	0.64 (0.53-0.74)	0.07	0.60	15.72	1.68	0.468 †
ELID_I	0.92 (0.89-0.94)	0.03	0.67	5.84	0.30	0.695	0.87 (0.81-0.91)	0.16	0.78	7.23	1.51	0.107

ELID_M	0.87 (0.81-0.90)	0.06	0.71	4.17	0.32	0.550	0.84 (0.78-0.89)	0.13	0.75	4.52	0.77	0.185
ELID_S	0.91 (0.87-0.94)	0.05	0.82	3.80	0.21	0.676	0.93 (0.90-0.95)	0.11	0.77	3.62	0.52	0.268
FPDI	0.73 (0.63-0.80)	0.01	0.48	10.31	0.29	0.828	0.73 (0.64-0.81)	0.06	0.59	12.04	1.23	0.430
EPDI_I	0.94 (0.91-0.96)	0.10	0.68	4.86	0.74	0.241	0.94 (0.91-0.96)	0.02	0.61	4.56	0.12	0.840
EPDI_M	0.90 (0.86-0.93)	0.08	0.68	3.53	0.40	0.380	0.67 (0.56-0.76)	0.14	1.33	7.03	0.73	0.421
EPDI_S	0.92	0.08	0.80	3.35	0.32	0.463	0.95	0.07	0.63	2.68	0.31	0.373

	(0.89-0.95)						(0.93-0.97)					
FExD	0.81 (0.73-0.86)	0.05	0.47	6.73	0.69	0.427	0.83 (0.77-0.88)	0.13	0.60	8.17	1.74	0.169 †
EExD_I	0.96 (0.94-0.97)	0.12	0.65	3.63	0.67	0.152	0.97 (0.96-0.98)	0.11	0.51	2.90	0.61	0.105
EExD_M	0.93 (0.91-0.95)	0.14	0.62	2.70	0.62	0.077	0.95 (0.93-0.96)	0.03	0.49	2.13	0.15	0.591
EExD_S	0.94 (0.91-0.96)	0.16	0.74	2.71	0.60	0.086	0.96 (0.95-0.97)	0.04	0.55	2.01	0.14	0.587
FExDI	0.70 (0.59-0.80)	0.16	0.65	13.87	3.51	0.050	0.79 (0.71-0.85)	0.00	0.48	11.03	0.07	0.960

EExDI_I	0.96 (0.95-0.98)	0.03	0.61	4.15	0.22	0.684	0.96 (0.95-0.98)	0.16	0.59	4.32	1.15	**0.039**
EExDI_M	0.95 (0.93-0.96)	0.02	0.60	3.06	0.10	0.801	0.95 (0.93-0.97)	0.10	0.53	2.86	0.54	0.144
EExDI_S	0.94 (0.92-0.96)	0.05	0.76	3.24	0.22	0.609	0.96 (0.94-0.97)	0.08	0.63	2.76	0.34	0.341
ID	0.83 (0.76-0.88)	0.06	0.21	1.74	0.47	**0.037**	0.90 (0.85-0.93)	0.03	0.15	1.22	0.27	0.085
EnD*	0.99 (0.90-1.00)	0.02	0.15	0.66	0.05	0.457 †	0.99 (0.99-1.0)	0.04	0.21	0.66	0.12	0.369 †
PD*	1.00	0.00	0.12	0.26	0.01	0.921	0.96	0.12	0.62	1.00	0.19	0.298

	(1.00-1.00)						(0.94-0.98)					
ExD*	0.99 (0.98-0.99)	0.11	0.37	0.42	0.13	0.241	0.99 (0.98-0.99)	0.04	0.52	0.57	0.04	0.692
Curvatures (mm)												
UPML	0.84 (0.78-0.88)	0.24	0.93	2.85	0.56	0.092	0.83 (0.75-0.88)	0.42	1.09	2.81	1.08	**0.002**
UPMLm	0.82 (0.75-0.87)	0.14	0.59	1.74	0.45	0.238	0.78 (0.70-0.84)	0.26	0.97	3.69	0.98	0.141 †
LPML	0.93 (0.91-0.95)	0.15	0.67	1.67	0.41	**0.042**	0.90 (0.86-0.93)	0.11	0.78	2.27	0.31	0.286
LPMLm	0.87	0.10	1.08	1.82	0.13	0.276	0.93	0.04	0.54	2.24	0.16	0.577

	(0.81-0.91)						(0.90-0.95)					
EL_I	0.96 (0.95-0.97)	0.08	1.52	2.15	0.32	0.585	0.94 (0.92-0.96)	0.09	1.32	2.22	0.15	0.617
EL_M	0.97 (0.96-0.98)	0.22	1.32	2.59	0.37	0.354 †	0.99 (0.98-0.99)	0.12	1.01	1.42	0.17	0.345
EL_S	0.98 (0.97-0.99)	0.25	1.75	4.15	0.37	0.138	0.99 (0.98-0.99)	0.08	0.92	1.33	0.11	0.513
Angles (°)												
MCA	0.84 (0.77-0.88)	0.58	1.90	4.61	1.05	**0.009**	0.86 (0.81-0.90)	0.23	1.74	4.05	0.55	0.298
MCAm	0.86	0.38	6.05	8.63	1.43	0.384	0.90	0.72	3.09	5.20	1.21	0.071

	(0.80-0.90)						(0.85-0.93)					
LCA	0.84 (0.77-0.88)	0.43	1.19	6.39	0.09	0.077	0.87 (0.82-0.91)	0.15	1.74	4.39	0.38	0.506
LCAm	0.68 (0.57-0.76)	1.00	0.74	13.16	0.06	0.201	0.82 (0.75-0.87)	0.18	4.03	6.42	0.29	0.730
CT	0.88 (0.84-0.92)	0.15	0.49	1.02	1.56	0.335	0.95 (0.92-0.96)	0.06	0.85	0.51	0.03	0.606
Mean	0.89	0.13	1.02	5.51	0.61		0.89	0.12	0.80	4.43	0.68	

CI, confidence interval

†represents p-values calculated from Wilcoxon's signed-rank test and the rest derived from paired-samples t-test. Results with P <0.05 are marked in bold.

Table 5. Inter-device reliability results of VECTRA M3 and H2 for periocular measurements

Device	**M3 vs H2**						**M2 vs H2 (Mean)**					
Comparison	**ICC (CI 95%)**	**MAD**	**TEM**	**rTEM**	**REM**	**p value**	**ICC (CI 95%)**	**MAD**	**TEM**	**rTEM**	**REM**	**p value**
Liner distances (mm)												
PFW	0.83 (0.46-0.93)	0.67	0.73	2.46	2.25	**<0.001**	0.82 (0.51-0.91)	0.65	0.76	2.55	2.20	**<0.001**
PFH	0.80 (0.70-0.86)	0.27	0.63	5.18	2.23	**0.001**	0.86 (0.81-0.90)	0.12	0.50	4.07	0.94	0.073
EEnD_I	0.79 (0.71-0.85)	0.33	0.88	5.31	1.98	**0.004**	0.85 (0.76-0.90)	0.39	0.73	4.39	2.32	**<0.001**

	0.88						0.92					
EEnD_M	(0.83-0.91)	0.18	0.78	3.27	0.74	0.080	(0.88-0.95)	0.22	0.61	2.58	0.93	**0.005**
	0.90						0.95					
EEnD_S	(0.87-0.93)	0.07	0.89	3.13	0.24	0.549	(0.93-0.96)	0.12	0.64	2.27	0.41	0.160
	0.66						0.72					
FPDm	(0.45-0.78)	0.45	0.69	15.10	9.86	**<0.001**	(0.48-0.84)	0.44	0.61	13.17	9.56	**<0.001**
	0.81						0.85					
EPDm_I	(0.73-0.86)	0.01	0.82	5.91	0.05	0.951	(0.79-0.90)	0.02	0.71	5.09	0.11	0.869
	0.86						0.90					
EPDm_M	(0.80-0.90)	0.27	0.76	3.60	1.26	**0.006**	(0.85-0.98)	0.23	0.66	3.11	1.08	**0.007**
	0.89						0.92					
EPDm_S	(0.84-0.92)	0.33	0.85	3.33	1.27	**0.003**	(0.88-0.95	0.27	0.73	2.83	1.05	**0.004**

							)					
FLmD	0.59 (0.46-0.70)	0.07	0.45	11.15	1.65	0.432	0.68 (0.57-0.77)	0.08	0.56	13.97	2.09	0.249
ELmD_I	0.77 (0.67-0.84)	0.38	0.94	8.77	3.53	**0.002** †	0.80 (0.72-0.86)	0.27	0.86	8.05	2.51	**0.005** †
ELmD_M	0.80 (0.73-0.86)	0.22	0.89	5.02	1.24	0.056	0.84 (0.78-0.88)	0.11	0.81	4.58	0.61	0.304
ELmD_S	0.85 (0.79-0.89)	0.12	0.99	4.48	0.55	0.346	0.88 (0.83-0.92)	0.02	0.90	4.04	0.10	0.848
FPD	0.69 (0.59-0.78)	0.13	0.60	17.29	3.86	0.108 †	0.73 (0.63-0.80)	0.18	0.55	15.61	5.18	**0.011** †
EPD_I	0.71 (0.54-	0.64	1.09	11.15	6.60	**<0.001** †	0.76 (0.63-	0.51	0.92	9.39	5.22	**<0.001** †

	0.81)						0.84)					
EPD_M	0.71 (0.58-0.79)	0.48	1.05	6.56	2.99	**<0.001**	0.77 (0.67-0.84)	0.39	0.91	5.68	2.44	**0.001**
EPD_S	0.81 (0.73-0.87)	0.43	1.16	5.65	2.08	**0.004**	0.85 (0.79-0.89)	0.34	1.04	5.04	1.62	**0.012**
FLID	0.63 (0.51-0.73)	0.04	0.64	16.85	1.00	0.962 †	0.73 (0.63-0.80)	0.05	0.51	13.42	1.36	0.552 †
ELID_I	0.83 (0.60-0.91)	0.78	1.00	8.98	6.97	**<0.001**	0.84 (0.64-0.92)	0.68	0.89	7.99	6.07	**<0.001**
ELID_M	0.74 (0.54-0.84)	0.66	0.98	5.86	3.93	**<0.001**	0.78 (0.61-0.87)	0.57	0.88	5.25	3.38	**<0.001**
ELID_S	0.84 (0.76-0.89)	0.48	1.06	4.94	2.26	**<0.001**	0.86 (0.80-0.90)	0.41	1.02	4.75	1.89	**0.002**

	0.45						0.56					
FPDI	(0.29-0.58)	0.27	0.82	17.27	5.68	0.074 †	(0.42-0.68)	0.23	0.64	13.52	4.92	**0.004**
	0.88						0.88					
EPDI_I	(0.82-0.92)	0.43	0.93	6.76	3.10	**<0.001**	(0.80-0.93)	0.49	0.89	6.51	3.53	**<0.001 †**
	0.60						0.74					
EPDI_M	(0.46-0.70)	0.44	1.51	7.94	2.32	**0.001 †**	(0.64-0.81)	0.41	1.09	5.71	2.15	**0.003**
	0.88						0.89					
EPDI_S	(0.83-0.91)	0.18	0.97	4.09	0.78	0.143	(0.85-0.92)	0.19	0.93	3.92	0.78	0.124
	0.45						0.53					
FExD	(0.28-0.59)	0.49	0.98	13.63	6.80	**0.004**	(0.36-0.66)	0.45	0.87	12.15	6.28	**<0.001**
	0.92						0.94					
EExD_I	(0.89-0.94)	0.20	0.86	4.85	1.11	0.077	(0.90-0.96)	0.31	0.76	4.29	1.75	**0.001**
EExD_M	0.90	0.11	0.72	3.11	0.46	0.255	0.91	0.19	0.68	2.93	0.84	**0.025**

	(0.86-0.93)						(0.87-0.94)					
	0.90						0.91					
EExD_S	(0.86-0.93)	0.05	0.88	3.26	0.17	0.686	(0.88-0.94)	0.11	0.84	3.08	0.40	0.315
FExDI	0.64 (0.42-0.77)	0.46	0.69	15.15	10.03	**<0.001** †	0.70 (0.51-0.81)	0.37	0.59	13.04	8.26	**<0.001**
EExDI_I	0.89 (0.43-0.96)	1.12	1.11	7.80	7.85	**<0.001**	0.89 (0.29-0.96)	1.18	1.09	7.71	8.31	**<0.001**
EExDI_M	0.87 (0.55-0.95)	0.84	0.61	3.21	4.41	**<0.001**	0.88 (0.43-0.96)	0.88	0.88	4.64	4.63	**<0.001**
EExDI_S	0.89 (0.79-0.94)	0.67	1.05	4.58	2.93	**<0.001**	0.90 (0.76-0.95)	0.74	0.97	4.23	3.20	**<0.001**
ID	0.85 (0.79-	0.02	0.19	1.57	0.15	0.454	0.87 (0.81-	0.06	0.17	1.39	0.52	**0.003**

	0.89)						0.91)					
EnD*	0.90 (0.98-0.99)	0.05	0.29	0.88	0.14	0.763 †	0.99 (0.99-1.0)	0.02	0.22	0.66	0.06	0.713 †
PD*	0.96 (0.93-0.98)	0.33	0.65	1.04	0.52	**0.005**	0.98 (0.92-0.99)	0.39	0.44	0.71	0.62	**<0.001**
ExD*	0.95 (0.65-0.98)	0.98	0.96	1.06	1.08	**<0.001**	0.96 (0.91-0.99)	0.90	0.90	1.00	1.00	**<0.001**
Curvatures (mm)												
UPML	0.76 (0.52-0.82)	1.02	1.37	3.56	2.66	**<0.001**	0.82 (0.68-0.89)	0.70	1.09	2.84	1.81	**<0.001**
UPMLm	0.65 (0.39-0.79)	1.00	1.38	5.34	3.87	**<0.001**	0.73 (0.48-0.85)	0.80	1.09	4.21	3.10	**<0.001**
LPML	0.87	0.68	1.11	3.28	1.99	**<0.00**	0.87	0.55	0.85	2.51	1.61	**<0.00**

	(0.69-0.93)					**1**	(0.75-0.92)					**1**
LPMLm	0.72 (0.27-0.87)	1.03	1.12	4.71	4.34	**<0.001**	0.75 (0.24-0.89)	0.96	1.00	4.21	4.05	**<0.001**
EL_I	0.89 (0.84-0.92)	0.16	1.89	3.18	0.27	0.519	0.92 (0.89-0.95)	0.16	1.51	2.54	0.27	0.406
EL_M	0.96 (0.94-0.97)	0.41	1.80	2.52	0.57	**0.048** †	0.97 (0.95-0.98)	0.36	1.65	2.32	0.50	0.096
EL_S	0.95 (0.92-0.96)	0.61	2.02	2.93	0.88	**0.020**	0.96 (0.94-0.97)	0.52	1.78	2.57	0.75	**0.023**
Angles (°)												
MCA	0.77 (0.64-0.85)	1.24	2.18	5.14	2.93	**<0.001**	0.84 (0.75-0.89)	0.84	1.75	4.12	1.96	**<0.001**
MCAm	0.79	1.86	4.32	7.11	3.06	**0.001**	0.83	2.41	3.76	6.20	3.98	**<0.00**

	(0.70-0.86)						(0.69-0.90)					**1**
LCA	0.71 (0.58-0.80)	1.22	2.61	6.49	3.04	**<0.001**	0.77 (0.58-0.86)	1.52	2.26	5.59	3.75	**<0.001**
LCAm	0.39 (0.11-0.58)	6.83	8.73	13.18	10.31	**<0.001**	0.47 (0.04-0.70)	7.42	7.81	11.76	11.17	**<0.001**
CT	0.79 (0.66-0.88	1.14	1.68	1.00	0.68	**<0.001**	0.84 (0.63-0.91)	1.09	1.46	0.87	0.65	**<0.001**
Mean	0.79	0.63	1.31	7.62	2.83		0.83	0.62	1.10	5.57	2.69	

CI, confidence interval

† represents p-values calculated from Wilcoxon's signed-rank test and the rest derived from paired-samples t-test.

Results with P <0.05 are marked in bold.

Table 6. Percentage of different periocular measurement variables in each reliability rating classification for VECTRA M3 and H2.

Variables	Upper lid fold-related variables (7/7)				Palpebral fissure-related variables (15/15)				Eyebrow-related variables (24/24)			
	M3-M3	H2-H2	M3-H2	M3-H2 (Mean)	M3-M3	H2-H2	M3-H2	M3-H2 (Mean)	M3-M3	H2-H2	M3-H2	M3-H2 (Mean)
ICC												
Excellent (⩾0.75)	71.4%(5/7)	57.1%(4/7)	0% (0/7)	0% (0/7)	93.3%(14/15)	100%(15/15)	73.3%(11/15)	86.7%(13/15)	100%(24/24)	95.8%(23/24)	83.3%(20/24)	95.8%(23/24)
Satisfactory (0.4–0.75)	28.6%(2/7)	42.9%(3/7)	100%(7/7)	100%(7/7)	6.7%(1/15)	0% (0/15)	20%(3/15)	13.3%(2/15)	0%(0/24)	4.2%(1/24)	16.7%(4/24)	4.2%(1/24)

Poor (<0.4)	0% (0/7)	0% (0/7)	0% (0/7)	0% (0/7)	0% (0/15)	0% (0/15)	6.7%(1/15)	0% (0/15)	0%(0/24)	0%(0/24)	0%(0/24)	0%(0/24)
MAD												
<1 unit	100%(7/7)	100%(7/7)	100%(7/7)	100%(7/7)	93.3%(14/15)	100%(15/15)	53.3%(8/15)	73.3%(11/15)	100%(24/24)	100%(24/24)	100%(24/24)	100%(24/24)
>1 unit	-	-	-	-	6.7%(1/15)	-	46.7%(7/15)	26.7(4/15)	-	-	-	-
TEM												
<1 unit	100%(7/7)	100%(7/7)	85.7%(6/7)	100%(7/7)	60%(9/15)	60%(9/15)	40%(6/15)	46.7%(7/15)	87.5%(21/24)	87.5%(21/24)	62.5%(15/24)	75%(18/24)
>1 unit	-	-	14.3%(1/7)	-	40%(6/15)	40%(6/15)	60%(9/15)	53.3%(8/15)	12.5%(3/24)	12.5%(3/24)	37.5%(9/24)	25%(6/24)
REM												

Excellent, (<1%)	57.1%(4/7)	28.6%(2/7)	-	-	73.3%(11/15)	80% (12/15)	26.7% (4/15)	33.3%(5/15)	95.8%(23/24)	87.5%(21/24)	41.7%(10/24)	45.8%(11/24)
Very good, (1–3.9%)	42.9%(3/7)	57.1%(4/7)	42.9%(3/7)	28.6%(2/7)	26.7% (4/15)	20% (3/15)	60%(9/15)	46.7%(7/15)	4.2%(1/24)	12.5%(3/24)	50%(12/24)	45.8%(11/24)
Good (4–6.9%)	0% (0/7)	14.3%(1/7)	28.6%(2/7)	42.9%(3/7)	-	-	6.7%(1/15)	6.7%(1/15)	-	-	4.2%(1/24)	8.3%(2/24)
Moderate, (7–9.9%)	-	-	14.3%(1/7)	28.6%(2/7)	-	-	-	-	-	-	4.2%(1/24)	-
Poor (>10%)	-	-	14.3%(1/7)	-	-	-	6.7%(1/15)	6.7%(1/15)	-	-	-	-
rTEM												
Excellent,	-	-	-	-	20% (3/15)	26.7%	46.7%(7/1	26.7%	-	-	-	

(<1%)						(4/15)	5)	(4/15)				
Very good, (1–3.9%)	-	-	-	-	46.7% (7/15)	40% (6/15)	26.7% (4/15)	26.7% (4/15)	75%(18/24)	70.8%(17/24)	37.5%(9/24)	41.7%(10/24)
Good (4–6.9%)	14.3%(1/7)	-	-	-	20% (3/15)	33.3% (5/15)	-	40%(6/15)	25%(6/24)	16.7%(4/24)	45.8%(11/24)	45.8%(11/24)
Moderate, (7–9.9%)	14.3%(1/7)	28.6%(2/7)	-	-	6.7%(1/15)	-	6.7%(1/15)	-	-	12.5%(3/24)	12.5%(3/24)	12.5%(3/24)
Poor (>10%)	71.4%(5/7)	71.4%(5/7)	100%(7/7)	100%(7/7)	6.7%(1/15)	-	6.7%(1/15)	6.7%(1/15)	-	-	4.2%(1/24)	-

4.9.3. Subtitle

4.1. ABSTRACT

4.2. INTRODUCTION

4.3. METHODS

4.4. RESULTS

4.5. DISCUSSION

4.6. CONCLUSIONS

4.7. DECLARATIONS

4.8. REFERENCES

4.9. APPENDIX

5. DISCUSSION

The publication of *Validation of the portable next-generation VECTRA H2 3D imaging system for periocular anthropometry* lays the foundation for future applications of portable 3d imaging systems in the periocular area. This study evaluated the differences in the reliability of two different 3D stereoscopic imaging devices used to quantify periocular morphology in Caucasian populations. To our knowledge, this is the first investigation to assess the reliability of portable 3D techniques in periocular anthropometry. Previous studies on periocular anthropometry have been based on static 3D imaging devices [57-60]. Therefore, the above study may facilitate the widespread use of portable devices in the study of periocular morphological changes. Static 3D stereophotogrammetry and landmark localization protocols are reliable (or precise) and accurate techniques for periocular anthropometry, the present study found that the reliability of portable devices for periocular measurements was generally consistent with that of static devices.

Existing studies have positively evaluated the reliability of both static and portable Vectra 3D imaging devices. Guo et al. verified the high reliability of the static VECTRA M3 stereophotogrammetric system for periocular anthropometric measurements, with the highest reliability for intra-measurer measurements, followed by inter-measurer and intra-device measurements[56]. In contrast, current studies of portable devices have focused on the face and have not assessed the reliability of periocular measurements. For this reason, this study compared the static device VECTRA M3 with the portable VECTRA H2 for periocular measurements. The results showed that the static device VECTRA M3 and the portable VECTRA H2 are the same in intra-device reliability metrics and even better in some cases for the H2. The inter-device reliability decreases compared to the intra-device, but the inter-device reliability improves when we take the average of the results of the two captured images. The intra-device reliability of VECTRA M3 in this study is consistent with the results of Guo et al. Both static and portable devices proved capable of obtaining accurate 3D images of the periocular area, but differences still existed between the systems. This difference may be because three consecutive acquisitions of the Vectra H2 may negatively affect the accuracy of the captured 3D images.

Forty-nine periocular data in the current study included 37 linear distances, seven curve distances, and five angles, mainly divided into eyelid fissure-related variables, upper eyelid fold-related variables, and eyebrow-related variables. The mean of M3 measurements ranged from 3.39-89.93 mm, or 40.93-168.33°, which is more consistent with the previous M3 measurements reported in the literature (4.02 to 90.72 mm or 36.41° to 166.77°);

and the mean of the current H2 measurement was 3.52-90.91 mm or 39.70-167.19°, which is also generally consistent with the above two measurements of M3. In the intra-device comparison for M3 there were no significant differences for the remaining 45 variables except for four variables PFH, ID, LPML, and MCA ($p < 0.001$, $p= 0.037$, $p= 0.042$, $p= 0.009$); while for H2 there were no statistically significant differences for the remaining 46 variables except for EPD_I, EExDI_I, and UPML ($p= 0.044$, $p= 0.039$, $p= 0.002$). When comparing between M3 and H2devices, all 34 variables were significantly different except for 15.

Since the portable Vectra H2 is being used for the first time for periocular measurements, a complete evaluation of the device's reliability is needed to prove its validity and reliability as a tool for periocular measurements. Reliability is one of the most commonly used metrics for evaluating anthropometric errors, indicating the degree to which repeated measurements give the same value. The main statistical methods commonly used in previous studies include ICC, MAD, REM, TEM, %TEM (or rTEM), total TEM, %total TEM, reliability coefficient (R), and Pearson correlation coefficient [7, 9, 10, 13-17]. Since the current study compared different variables and between different devices, only the first five statistical metrics were calculated to analyze the reliability of periocular measurements. Previous studies have investigated the high intra- and inter-measurer reliability of the Vectra M3 device, so the current study focused on the intra- and inter-device reliability of the two different devices.

Overall, our results show that intra-device reliability is largely consistent and highest for M3 and H2: MAD (0.13 and 0.12 units), REM (0.61 and 0.68%), TEM (1.02 and 0.80 units), rTEM (5.51 and 4.43%), and ICC (0.89 and 0.89). The next comparison is between M3 and H2 devices, with values of 0.63 units, 2.83%, 1.31 units, 7.62%, and 0.79 for MAD, REM, TEM, rTEM, and ICC, respectively. Reliability is somewhat improved when using the average of the two captured image measurements for H2 and M3, with values of 0.62 units, 2.69%, 1.10 units, 5.57%, and 0.83%, respectively. This lower inter-device reliability may be because, in addition to calibration errors, subject repositioning errors, and landmark positioning errors, photographic errors from different devices were added to the inter-device errors.

Previous literature has reported that smaller measurements typically have lower mean absolute difference (MAD) and technical error of measurement (TEM) estimates and higher relative error of measurement (REM) estimates[61, 62]. The upper eyelid folds variables in this study had the smallest values of measurements (M3: 3.77-6.93 units, H2: 3.52-7.42 units), followed by eyebrow-related variables (M3: 10.08-70.96 units, H2: 9.43-71.37 units) and palpebral fissure related variables (M3: 11.91-168.33 units, H2: 11.90- 167.19 units). Thus,

eyelid fold-related variables showed the lowest MAD, TEM, and highest REM, rTEM; they had moderate or poor intra-device reliability, and poor inter-device reliability. The eyebrow-related variables showed slightly higher MAD and TEM but slightly lower REM and rTEM; they all had very good or good intra-device reliability and good inter-device reliability. The eyelid fissure-related variables had the maximum MAD and TEM correspondingly, the REM and rTEM were relatively minimal; their intra- and inter-device reliability was excellent or very good or good. Overall, the lid fissure-related variables had the highest reliability, followed by the eyebrow-related variables, and the upper eyelid folds variables. The above results are more consistent with Guo et al.'s evaluation of the intra-rater, inter-rater, and intra-method reliability of these three categories of periocular variables[56].

There are some limitations to this study. As children and disabled people cannot ensure they remain still during photography, only healthy Caucasian adults who are easy to cooperate with were included in this study. All photographs in this study were captured indoors in the exact fixed location, underutilizing the portability feature of the VECTRA H2 device. The data measured were linear distances, curves, and angles around the eye, without measuring the area and volume, another advantage of the 3d camera. Thus, future studies could evaluate the reliability of portable 3D devices in people of different ages, races, and health conditions, in different locations and environments (e.g., hospital rooms, operating rooms, outdoors), and for the periocular area and volume measurements.

6.REFERENCES

1. Fan W, Guo Y, Hou X, Liu J, Li S, Ju S, et al. Validation of the Portable Next-Generation VECTRA H2 3D Imaging System for Periocular Anthropometry. Front Med (Lausanne). 2022;9:833487.

2. Tur JA, Bibiloni MDM. Anthropometry, Body Composition and Resting Energy Expenditure in Human. Nutrients. 2019;11(8).

3. Eveleth PB. Physical status: the use and interpretation of anthropometry. Report of a WHO Expert Committee. Wiley Online Library; 1996.

4. Farkas LG. Anthropometry of the Head and Face: Lippincott Williams & Wilkins; 1994.

5. Kolar JC. Methods in anthropometric studies. Cleft Palate Craniofac J. 1993;30(4):429-31.

6. Kolar JC. An epidemiological study of nonsyndromal craniosynostoses. J Craniofac Surg. 2011;22(1):47-9.

7. Kolar JC, Salter EM, Weinberg SM. Preoperative craniofacial dysmorphology in isolated sagittal synostosis: a comprehensive anthropometric evaluation. J Craniofac Surg. 2010;21(5):1404-10.

8. Metzler P, Zemann W, Jacobsen C, Grätz KW, Obwegeser JA. Postoperative cranial vault growth in premature sagittal craniosynostosis. J Craniofac Surg. 2013;24(1):146-9.

9. Metzler P, Zemann W, Jacobsen C, Grätz KW, Obwegeser JA. Cranial vault growth patterns of plagiocephaly and trigonocephaly patients following fronto-orbital advancement: a long-term anthropometric outcome assessment. J Craniomaxillofac Surg. 2013;41(6):e98-e103.

10. Fearon JA, Ruotolo RA, Kolar JC. Single sutural craniosynostoses: surgical outcomes and long-term growth. Plast Reconstr Surg. 2009;123(2):635-42.

11. Farkas LG, Hreczko TA, Kolar JC, Munro IR. Vertical and horizontal proportions of the face in young adult North American Caucasians: revision of neoclassical canons. Plast Reconstr Surg. 1985;75(3):328-38.

12. Farkas LG, Hreczko TM, Katic MJ, Forrest CR. Proportion indices in the craniofacial regions of 284 healthy North American white children between 1 and 5 years of age. J Craniofac Surg. 2003;14(1):13-28.

13. Masoud MI, Bansal N, J CC, Manosudprasit A, Allareddy V, Haghi A, et al. 3D dentofacial photogrammetry reference values: a novel approach to orthodontic diagnosis. Eur J Orthod. 2017;39(2):215-25.

14. Manosudprasit A, Haghi A, Allareddy V, Masoud MI. Diagnosis and treatment planning of orthodontic patients with 3-dimensional dentofacial records. Am J Orthod Dentofacial Orthop. 2017;151(6):1083-91.

15. Hanawa S, Kitaoka A, Koyama S, Sasaki K. Influence of maxillary obturator prostheses on facial morphology in patients with unilateral maxillary defects. J Prosthet Dent. 2015;113(1):62-70.

16. Mertens C, Wessel E, Berger M, Ristow O, Hoffmann J, Kansy K, et al. The value of three-dimensional photogrammetry in isolated sagittal synostosis: Impact of age and surgical technique on intracranial volume and cephalic index—a retrospective cohort study. J Craniomaxillofac Surg. 2017;45(12):2010-6.

17. Choi JW, Lee JY, Oh TS, Kwon SM, Yang SJ, Koh KS. Frontal soft tissue analysis using a 3 dimensional camera following two-jaw rotational orthognathic surgery in skeletal class III patients. J Craniomaxillofac Surg. 2014;42(3):220-6.

18. Jung J, Lee CH, Lee JW, Choi BJ. Three dimensional evaluation of soft tissue after orthognathic surgery. Head Face Med. 2018;14(1):21.

19. Terzic A, Schouman T, Scolozzi P. [Accuracy of morphological simulation for orthognatic surgery. Assessment of a 3D image fusion software]. Rev Stomatol Chir Maxillofac Chir Orale. 2013;114(4):276-82.

20. Verhulst A, Hol M, Vreeken R, Becking A, Ulrich D, Maal T. Three-Dimensional Imaging of the Face: A Comparison Between Three Different Imaging Modalities. Aesthet Surg J. 2018;38(6):579-85.

21. Hermans DJ, Maal TJ, Bergé SJ, van der Vleuten CJ. Three-dimensional stereophotogrammetry: a novel method in volumetric measurement of infantile hemangioma. Pediatr Dermatol. 2014;31(1):118-22.

22. Baik HS, Jeon JM, Lee HJ. Facial soft-tissue analysis of Korean adults with normal occlusion using a 3-dimensional laser scanner. Am J Orthod Dentofacial Orthop. 2007;131(6):759-66.

23. Kau CH, Hunter LM, Hingston EJ. A different look: 3-dimensional facial imaging of a child with Binder syndrome. Am J Orthod Dentofacial Orthop. 2007;132(5):704-9.

24. Kau CH, Zhurov A, Richmond S, Bibb R, Sugar A, Knox J, et al. The 3-dimensional construction of the average 11-year-old child face: a clinical evaluation and application. J Oral Maxillofac Surg. 2006;64(7):1086-92.

25. Hutton TJ, Buxton BF, Hammond P, Potts HW. Estimating average growth trajectories in shape-space using kernel smoothing. IEEE Trans Med Imaging. 2003;22(6):747-53.

26. Tremp M, di Summa PG, Schaakxs D, Oranges CM, Wettstein R, Kalbermatten DF. Nipple Reconstruction After Autologous or Expander Breast Reconstruction: A Multimodal and 3-Dimensional Analysis. Aesthet Surg J. 2017;37(2):179-87.

27. Farkas LG, Posnick JC, Hreczko TM. Anthropometric growth study of the head. Cleft Palate Craniofac J. 1992;29(4):303-8.

28. Wong JY, Oh AK, Ohta E, Hunt AT, Rogers GF, Mulliken JB, et al. Validity and reliability of

craniofacial anthropometric measurement of 3D digital photogrammetric images. Cleft Palate Craniofac J. 2008;45(3):232-9.

29. Gavan JA, Washburn SL, Lewis PH. Photography: an anthropometric tool. Am J Phys Anthropol. 1952;10(3):331-53.

30. Edler R, Wertheim D, Greenhill D. Comparison of radiographic and photographic measurement of mandibular asymmetry. Am J Orthod Dentofacial Orthop. 2003;123(2):167-74.

31. Lin CS, Shaari R, Alam MK, Rahman SA. Photogrammetric analysis of nasolabial angle and mentolabial angle norm in Malaysian adults. Bangladesh Journal of Medical Science. 2013;12(2):209-19.

32. Packiriswamy V, Kumar P, Rao KG. Photogrammetric analysis of palpebral fissure dimensions and its position in malaysian South Indian ethnic adults by gender. N Am J Med Sci. 2012;4(10):458-62.

33. Milosević SA, Varga ML, Slaj M. Analysis of the soft tissue facial profile of Croatians using of linear measurements. J Craniofac Surg. 2008;19(1):251-8.

34. Kale-Varlk S. Angular photogrammetric analysis of the soft tissue facial profile of Anatolian Turkish adults. J Craniofac Surg. 2008;19(6):1481-6.

35. Beugre JB, Diomande M, Assi AR, Koueita MK, Vaysse F. Angular photogrammetric analysis and evaluation of facial esthetics of young Ivorians with normal dental occlusion. Int Orthod. 2017;15(1):25-39.

36. Dindaroğlu F, Kutlu P, Duran GS, Görgülü S, Aslan E. Accuracy and reliability of 3D stereophotogrammetry: A comparison to direct anthropometry and 2D photogrammetry. Angle Orthod. 2016;86(3):487-94.

37. Jacobs RA. Three-dimensional photography. Plast Reconstr Surg. 2001;107(1):276-7.

38. Hajeer MY, Millett DT, Ayoub AF, Siebert JP. Applications of 3D imaging in orthodontics: part I. J Orthod. 2004;31(1):62-70.

39. Al-Omari I, Millett DT, Ayoub AF. Methods of assessment of cleft-related facial deformity: a review. Cleft Palate Craniofac J. 2005;42(2):145-56.

40. Brons S, van Beusichem ME, Bronkhorst EM, Draaisma J, Bergé SJ, Maal TJ, et al. Methods to quantify soft-tissue based facial growth and treatment outcomes in children: a systematic review. PLoS One. 2012;7(8):e41898.

41. Kochel J, Meyer-Marcotty P, Strnad F, Kochel M, Stellzig-Eisenhauer A. 3D soft tissue analysis--part 1: sagittal parameters. J Orofac Orthop. 2010;71(1):40-52.

42. Othman SA, Majawit LP, Wan Hassan WN, Wey MC, Mohd Razi R. Anthropometric Study of Three-Dimensional Facial Morphology in Malay Adults. PLoS One. 2016;11(10):e0164180.

43. Verhoeven TJ, Coppen C, Barkhuysen R, Bronkhorst EM, Merkx MA, Bergé SJ, et al. Three dimensional evaluation of facial asymmetry after mandibular reconstruction: validation of a new method using stereophotogrammetry. Int J Oral Maxillofac Surg. 2013;42(1):19-25.

44. Erten O, Yılmaz BN. Three-Dimensional Imaging in Orthodontics. Turk J Orthod. 2018;31(3):86-94.

45. Metzler P, Sun Y, Zemann W, Bartella A, Lehner M, Obwegeser JA, et al. Validity of the 3D VECTRA photogrammetric surface imaging system for cranio-maxillofacial anthropometric measurements. Oral Maxillofac Surg. 2014;18(3):297-304.

46. Modabber A, Peters F, Kniha K, Goloborodko E, Ghassemi A, Lethaus B, et al. Evaluation of the accuracy of a mobile and a stationary system for three-dimensional facial scanning. J Craniomaxillofac Surg. 2016;44(10):1719-24.

47. de Menezes M, Rosati R, Ferrario VF, Sforza C. Accuracy and reproducibility of a 3-dimensional stereophotogrammetric imaging system. J Oral Maxillofac Surg. 2010;68(9):2129-35.

48. Andrade LM, Rodrigues da Silva AMB, Magri LV, Rodrigues da Silva MAM. Repeatability Study of Angular and Linear Measurements on Facial Morphology Analysis by Means of Stereophotogrammetry. J Craniofac Surg. 2017;28(4):1107-11.

49. Othman SA, Ahmad R, Mericant AF, Jamaludin M. Reproducibility of facial soft tissue landmarks on facial images captured on a 3D camera. Aust Orthod J. 2013;29(1):58-65.

50. Othman SA, Saffai L, Wan Hassan WN. Validity and reproducibility of the 3D VECTRA photogrammetric surface imaging system for the maxillofacial anthropometric measurement on cleft patients. Clin Oral Investig. 2020;24(8):2853-66.

51. Verhulst A, Hol M, Vreeken R, Becking A, Ulrich D, Maal T. Three-Dimensional Imaging of the Face: A Comparison Between Three Different Imaging Modalities. Aesthetic Surgery Journal. 2018;38(6):579-85.

52. Camison L, Bykowski M, Lee WW, Carlson JC, Roosenboom J, Goldstein JA, et al. Validation of the Vectra H1 portable three-dimensional photogrammetry system for facial imaging. Int J Oral Maxillofac Surg. 2018;47(3):403-10.

53. Gibelli D, Pucciarelli V, Cappella A, Dolci C, Sforza C. Are Portable Stereophotogrammetric Devices Reliable in Facial Imaging? A Validation Study of VECTRA H1 Device. J Oral Maxillofac Surg. 2018;76(8):1772-84.

54. Liberton DK, Mishra R, Beach M, Raznahan A, Gahl WA, Manoli I, et al. Comparison of Three-Dimensional Surface Imaging Systems Using Landmark Analysis. J Craniofac Surg. 2019;30(6):1869-72.

55. Hammond P, Hutton TJ, Allanson JE, Buxton B, Campbell LE, Clayton-Smith J, et al. Discriminating power of localized three-dimensional facial morphology. Am J Hum Genet. 2005;77(6):999-1010.

56. Guo Y, Rokohl AC, Schaub F, Hou X, Liu J, Ruan Y, et al. Reliability of periocular anthropometry using three-dimensional digital stereophotogrammetry. Graefes Arch Clin Exp Ophthalmol. 2019;257(11):2517-31.

57. Guo Y, Hou X, Rokohl AC, Jia R, Heindl LM. Reliability of Periocular Anthropometry: A Comparison of Direct, 2-Dimensional, and 3-Dimensional Techniques. Dermatol Surg. 2020;46(9):e23-e31.

58. Guo Y, Schaub F, Mor JM, Jia R, Koch KR, Heindl LM. A Simple Standardized Three-Dimensional Anthropometry for the Periocular Region in a European Population. Plast Reconstr Surg. 2020;145(3):514e-23e.

59. Liu J, Rokohl AC, Guo Y, Li S, Hou X, Fan W, et al. Reliability of Stereophotogrammetry for Area Measurement in the Periocular Region. Aesthetic Plast Surg. 2021;45(4):1601-10.

60. Liu J, Guo Y, Arakelyan M, Rokohl AC, Heindl LM. Accuracy of Areal Measurement in the Periocular Region Using Stereophotogrammetry. J Oral Maxillofac Surg. 2021;79(5):1106.e1-.e9.

61. Andrade LM, Rodrigues da Silva AMB, Magri LV, Rodrigues da Silva MAM. Repeatability Study of Angular and Linear Measurements on Facial Morphology Analysis by Means of Stereophotogrammetry. Journal of Craniofacial Surgery. 2017;28(4):1107-11.

62. Weinberg SM, Scott NM, Neiswanger K, Brandon CA, Marazita ML. Digital Three-Dimensional Photogrammetry: Evaluation of Anthropometric Precision and Accuracy Using a Genex 3D Camera System. The Cleft Palate-Craniofacial Journal. 2004;41(5):507-18.

7. APPENDIX

7.1 Subtitles

3.1 Anthropometry of facial soft tissues

3.2 Different techniques for Anthropometry

3.3 Different devices for Three-dimensional (3D) stereophotogrammetry

3.4 Current research on Three-dimensional (3D) stereophotogrammetry for periocular anthropometry

3.5 Aims

4.1. ABSTRACT

4.2. INTRODUCTION

4.3. METHODS

4.4. RESULTS

4.5. DISCUSSION

4.6. CONCLUSIONS

4.7. DECLARATIONS

4.8. REFERENCES

4.9. APPENDIX

8. VORABVERÖFFENTLICHUNGEN VON ERGEBNISSEN

1. **Fan W**, Guo Y, Hou X, Liu J, Li S, Ju S, et al. Validation of the Portable Next-Generation VECTRA H2 3D Imaging System for Periocular Anthropometry. Front Med (Lausanne). 2022;9:833487.

Presentation

1. **Wanlin Fan,** Alexander C. Rokohl, Patrick Kupka, Xiaoyi Hou, Jinhua Liu, Senmao Li, Adam Kopecky, Sitong Ju, Philomena A. Wawer Matos, Yongwei Guo, Ludwig M. Heind (2022). *Quantitative volumetric study of different periocular tumor models.* 15-17. Sep. 2022 – 40th Annual Meeting of the European Society of Ophthalmic Plastic and Reconstructive Surgery in NICE.